Student thesis series INES nr 551

Influence of permafrost disintegration on wetland carbon fluxes in Abisko, Sweden

Aida Esmailzadeh Davani

2021
Department of
Physical Geography and Ecosystem Science
Lund University
Sölvegatan 12
S-223 62 Lund
Sweden

Aida Esmailzadeh Davani (2021).
Influence of permafrost disintegration on wetland carbon fluxes in Abisko, Sweden

Effekter av tinande permafrost på kolutbytet av våtmarker i Abisko, Sverige
Master degree thesis, 30 credits in *Physical Geography and Ecosystem Analysis*
Department of Physical Geography and Ecosystem Science, Lund University

Level: Master of Science (MSc)

Course duration: *January* 2021 until *June* 2021

Disclaimer

Influence of permafrost disintegration on wetland carbon fluxes in Abisko, Sweden

---

Aida Esmailzadeh Davani

Master thesis, 30 credits, in *Physical Geography and Ecosystem Analysis*

Supervisors
Lena Ström
Dep. of Physical Geography and Ecosystem Science, Lund University

Joel White
Dep. of Physical Geography and Ecosystem Science, Lund University

Exam committee
Thomas Pugh
Dep. of Physical Geography and Ecosystem Science, Lund University

Mayra Rulli
Dep. of Physical Geography and Ecosystem Science, Lund University

Acknowledgements

I would like to thank my two supervisors: Lena Ström and Joel White. Thank you for allowing me to take part of your data for my master thesis. But most of all, thank you for the immense support and excellent supervision, as well as the valuable advice along the way! Writing this thesis would not have been possible without the two of you.

I would also like to thank my fellow classmates and friends for all your support, not only during my thesis-writing, but also throughout this whole master's.

Abstract

The northern permafrost regions are experiencing a rapid warming as surface temperatures are rising, causing a disintegration of permafrost and a deepening of the active layer (AL). This releases previously frozen carbon, making it available for decomposition by microbes. The combination of the high microbial activity and overall wetter soils may cause anoxic conditions and in turn methane (CH_4) and carbon dioxide (CO_2) release into the atmosphere, further contributing to warming of the climate. The main drivers, and therefore, the magnitude of CO_2 and CH_4 fluxes may vary spatially (CO_2/CH_4). Thus, the aim of this study is to investigate the influence of spatial variability of site-specific conditions such as vegetation composition, AL depth, water table depth (WTD) on the magnitude of carbon fluxes (CO_2/CH_4) between and within sites. Multiple replicate measurements of CO_2 and CH_4 concentrations, WTD, AL depth, air temperature (T_{air}) and soil temperature (T_{soil}) were taken from three different locations in Abisko, Sweden. The three study sites had varying stages of permafrost degradation: Storflaket had a relative stable permafrost, Kursflaket is currently undergoing permafrost degradation and Katterjokk has undergone a complete permafrost loss over last few decades. The results showed significant differences in CO_2 and CH_4 fluxes between and within the sites. The CH_4 emissions and CO_2 uptake were significantly higher in the site with completely disintegrated permafrost (Katterjokk), compared to the other two sites with permafrost presence. CH_4 fluxes were also significantly higher for wet plots, compared to dry plots. The CH_4 emissions were shown to be mainly driven by the WTD and AL depth as well as the abundance of aerenchymateous vegetation. No significant relationship between the investigated variables and CO_2 fluxes could be found. However, there was a significant difference in ecosystem respiration (R_{eco}) between the wet and dry plots, indicating that there may be a relationship between WTD and CO_2. The results demonstrated that even within the Abisko region, there were considerable variations in carbon fluxes as well as drivers of the fluxes between and within the sites. The differences in carbon fluxes and the site-specific conditions are important to take into consideration when extrapolating and generalising for larger areas. Furthermore, a continued disintegration of permafrost and deepening of the AL, may further alter the sub arctic ecosystem of Abisko and thereby enhance the spatial variability, as site-specific conditions continue to change. Moreover, further permafrost disintegration on a global scale may lead to even more CH_4 emissions, amplifying the initial warming.

Keywords: *Physical Geography, Ecosystem Analysis, Permafrost, CH_4 flux, CO_2 flux, Abisko, Wetlands*

Table of Contents

List of abbreviations

AL	Active layer
CH_4	Methane
CO_2	Carbon dioxide
GHG	Greenhouse gas
GPP	Gross primary production ($GPP = R_{eco} - NEE$)
NEE	Net ecosystem exchange (CO_2 light)
R_a	Autotrophic respiration
R_{eco}	Ecosystem respiration (CO_2 dark) ($R_{eco} = R_a + R_h$)
R_h	Heterotrophic respiration
T_{air}	Air temperature
T_{soil}	Soil temperature
WTD	Water table depth (cm below surface)

1. Introduction

Over recent decades the global atmospheric methane (CH_4) concentration has rapidly increased and is currently approximately 2.6 times higher than preindustrial levels (Nisbet et al. 2014; Schaefer et al. 2016; Dean et al. 2018; Saunois et al. 2020). The sources of CH_4 emission are both natural and anthropogenic, with the largest source being agriculture and waste, accounting for ca. 34 % of the total emissions, followed by natural wetlands, which accounts for approximately 30 % of the total emissions and are the largest natural source of CH_4 (Dean et al. 2018). Out of the total wetland emissions, northern wetlands represent 34 % (Wang et al. 1996). Furthermore, the northern permafrost region constitutes approximately 50% of the global below-ground carbon storage (Tarnocai et al. 2009; McCalley et al. 2014).

With rising global temperatures, the northern permafrost region is experiencing a rapid warming as surface temperatures are increasing and precipitation patterns are changing (IPCC 2019). This is impacting the arctic permafrost extent, as the warming is causing a disintegration of the permafrost and consequently deepening active layers (AL) (Svensson et al. 1999; Christensen et al. 2004; Ström and Christensen 2007; Johansson et al. 2011; Olefeldt et al. 2013; Romanovsky et al. 2017; IPCC 2019). This is in turn changing the hydrological and biogeochemical conditions of the landscape as the soil is becoming wetter and previously frozen carbon is released and available for decomposition by microbes (Svensson et al. 1999; Christensen et al. 2004; Ström and Christensen 2007; Olefeldt et al. 2013; IPCC 2019). The combination of waterlogged soils and high decomposition rates causes anoxic conditions and may in turn lead to CH_4 release (Svensson et al. 1999; Christensen et al. 2004; Ström and Christensen 2007; Olefeldt et al. 2013). This transfer of carbon, in the form of CH_4 and carbon dioxide emissions (CO_2), from the soil into the atmosphere, magnifies the initial warming and in turn causes a so called “arctic amplification” of the warming (Christensen et al. 2004; Malmer et al. 2005; Ström and Christensen 2007; Åkerman and Johansson 2008; Schuur et al. 2013).

The Abisko region in subarctic Sweden is a well-researched area and has been the subject of permafrost and greenhouse gas (GHG) studies over recent decades (Christensen et al. 2004; Malmer et al. 2005; Åkerman and Johansson 2008; Metcalf et al. 2018). In this area the disintegration of permafrost has resulted in a deeper AL and overall wetter soil conditions through the release of nutrient-rich water (Christensen et al. 2004; Malmer et al. 2005). This has in turn caused a shift in the species composition in the area, as over the last decades an expansion of graminoid vegetation has been observed. Certain graminoid species enable CH_4 transport through their

aerenchymateous tissue, which further amplifies the GHG emissions in the area (Christensen et al. 2004; Malmer et al. 2005; Åkerman and Johansson 2008).

Numerous studies indicate that the main drivers of CH_4 production typically are ground temperature, water table depth (WTD), topography, snow cover and vegetation composition (Torn and Chapin 1993; Christensen et al. 2004; Kotsyurbenko et al. 2004; Johansson et al. 2006; Ström and Christensen 2007). As these parameters may vary between locations, it may therefore also influence the CH_4 production and emission (Johansson et al. 2006). Thus, the aim of this study will be to investigate the influence of spatial variability of site-specific conditions between and within sites on carbon fluxes (CO_2/CH_4). More specifically, by what magnitude are the carbon fluxes varying between and within the study sites? Is the change mainly determined by vegetation composition, AL depth, WTD or are there other main drivers? In order to address these question, multiple measurements have been taken from three different wetland locations in Abisko with varying stages of permafrost degradation.

Main hypotheses:

h_0: There is no difference in carbon fluxes (CO_2/CH_4) between the study sites or the individual plots.

h_1: Sites and plots with higher abundance of aerenchymateous species will generate higher carbon fluxes (CO_2/CH_4).

h_2: Sites and plots with a deeper active layer depth will generate higher carbon fluxes (CO_2/CH_4).

h_3: Sites and plots with a higher water table will generate higher carbon fluxes (CO_2/CH_4).

2. Background

2.1. Arctic permafrost regions and landforms

Permafrost most commonly occurs in regions where the mean annual temperature is below 0 °C and is generally defined as “ground that remains at or below 0 °C for at least two consecutive years” (Dobinski 2011). Therefore, permafrost is usually constrained to either alpine regions where temperature are low due to the high altitudes or arctic and Antarctic regions where temperatures are low due to the high latitudes

(Dobinski 2011). Permafrost consists of an upper layer of soil that thaws and freezes seasonally, this is typically referred to as the AL i.e., the depth from the surface to the permafrost. Furthermore, permafrost is typically divided into three main categories: continuous, discontinuous, and sporadic permafrost. A continuous permafrost implies that 90-100% of the surface is underlaid by permafrost, discontinuous permafrost means that 50-90% of the surface is underlaid by permafrost and sporadic permafrost entails 10-50% of the surface (Johansson et al. 2006).

There are a number of landforms typically associated with a permafrost landscape. In discontinuous permafrost regions palsas are commonly formed (Seppälä 1982; Kujala et al. 2008). These are formed as a result of the thermal properties of peat (Seppälä 1982; Kujala et al. 2008). The low winter temperatures allow deep freezing of the peat from above and in the summer the same peat insulates against the summer heat. This allows formation of an ice core inside the peat that continuous to grow (Seppälä 1982; Kujala et al. 2008). As the ice core grows, the overlying layer is lifted, creating cracks in the soil as well as water accumulation around the edges (Seppälä 1982). Pingo is another common landform mostly associated with continuous permafrost regions (Seppälä 1982). Pingos are larger than palsas and are formed when water rises through hydraulic pressure through gaps in the permafrost (Seppälä 1982). This water eventually freezes and forms ice cores which expands and lifts the overlying soil in a similar manner as in palsas, with the main difference being that in this case the freezing takes place from below (Seppälä 1982). Thermokarst lakes is another landform commonly observed in permafrost regions. These are formed when lenses of ice in the permafrost melts, thereby causing the ground to subside and subsequently forming an irregular surface with thermokarst lakes (Seppälä 2006).

Northern Scandinavia and subarctic Sweden is characterized by discontinuous and sporadic permafrost. In northern Sweden permafrost is mostly found in mires in the form of palsas and peat plateaus (Gisnås et al. 2016).

2.2. Permafrost and climate change

The northern permafrost regions are believed to have been developed during Holocene as carbon accumulated slowly over thousands of years (MacDonald et al. 2006). The slow accumulation of carbon and subsequent formation of peat is a result of the cool regional temperatures causing a deceleration of decomposition by microbes (Ovenden 1990). Throughout Holocene the northern permafrost regions has acted as a net carbon sink (Loisel et al. 2014; Lindgren et al. 2018). Currently, approximately 17% of the Earth's surface and 22% of the northern hemisphere is underlain by permafrost and the

northern permafrost region alone constitutes about 50% of the global below ground carbon storage (Tarnocai et al. 2009; Gruber 2011; Biskaborn et al. 2019). This is approximately equivalent to 1460-1600 petagrams (Schuur et al. 2018), making the northern circumpolar permafrost regions an important carbon storage (Tarnocai et al. 2009).

Rising global temperatures are threating the long-term carbon storage in the northern peatlands, as increasing surface temperatures and changes in precipitation patterns are causing the permafrost to disintegrate (Hawkins and Sutton 2012; Fyfe et al. 2013; IPCC 2019). In addition, changes in the climate in high latitudes are typically amplified due to so called positive feedback-effects (Figure 1). This is in turn causing a quite rapid acceleration of the northern permafrost disintegration (Joabsson et al. 1999; Hawkins and Sutton 2012; IPCC 2019).

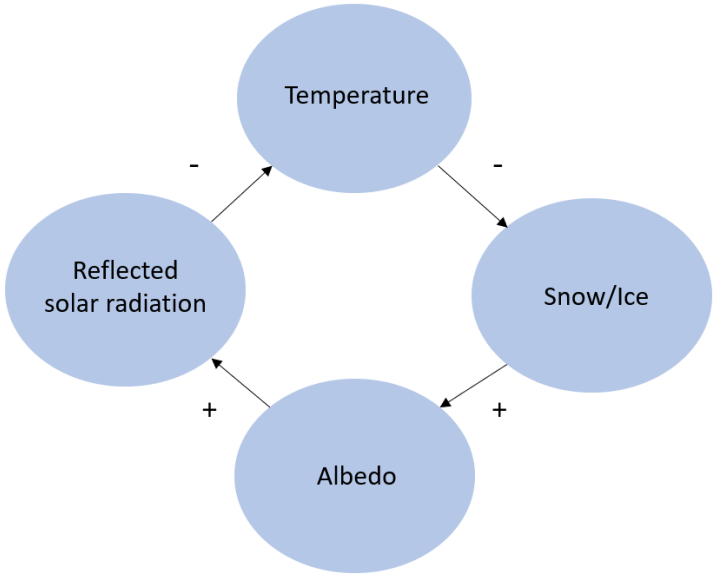

Figure 1. Scheme showing the positive feedback cycle of snow and ice albedo. The arrows indicate the direction of change, and the signs indicate either a decrease (-) or increase (+) of the respective change.

Johansson et al. (2006) have identified a number of physical and climatic parameters that have a substantial impact on the distribution of permafrost in subarctic northern Sweden. The ground temperature is the main driver, therefore factors that influence the ground temperature such as topography, soil type, wind, and snow cover, do in turn also have an effect on the permafrost distribution (Johansson et al. 2006). Furthermore, snow cover was singled out as one of the most influential parameters impacting the presence of permafrost (Johansson et al. 2006). The snow serves as an insulator that both prevents heat loss from the ground as well as penetration of cold winter air into the ground, consequently causing an increase in surface temperatures (Johansson et al. 2006). The snow depth has been projected to increase in the Abisko region (Sælthun and Barkved

2003). Additionally, higher surface temperatures are causing a reduction of the arctic spring snow cover extent and duration (Hawkins and Sutton 2012; Fyfe et al. 2013; IPCC 2019). Less snow cover in the spring may in turn initiate positive feedbacks where the lower albedo of the surface causes further warming as less shortwave radiation is reflected back to the atmosphere (Figure 1) (Hall 2004; Serreze and Francis 2006). Thereby, the increasing snow depth in combination with the lack of snow cover in spring causes even warmer surface temperatures and in turn a disintegration of permafrost (Johansson et al. 2006).

Similarly, the disintegration of permafrost and subsequent CH_4 release into the atmosphere may contribute to further warming as more GHGs are released into the atmosphere, amplifying the initial warming (Johansson et al. 2006; Dean et al. 2018). According to the IPCC (2019), trends indicate increased AL-depths and a loss of up to ca 90 % of near-surface permafrost by the year 2100, following RCP8.5 (IPCC 2019).

A disintegration of the permafrost and thereby a deepening of the AL causes a physical alteration of the environment, as the previously frozen ground subsides (Dobinski 2011). This shifts the landscape from a more elevated dryer ombrotrophic ecosystem (main water-input from precipitation) to an overall wetter more nutrient-rich minerotrophic landscape (main water-input from precipitation and surroundings) (Svensson et al. 1999; Dean et al. 2018). Moreover, this also causes a shift in the vegetation composition from shrub dominated to more sedge rich vegetation (Christensen et al. 2004; Malmer et al. 2005). The increasing AL also have an influence of the hydrology of the area. The absence of permafrost allows surface water to penetrate deeper into the soil, vertically, as well as move laterally in ways that may not have been possible with permafrost still present. This in turn may influence the ground water storage and the runoff of water (Walvoord and Kurylyk 2016).

2.3. Land and atmosphere exchange of carbon

2.3.1. CH_4 production and transport

As permafrost begins to disintegrate due to the increasing northern temperatures, carbon that was previously frozen and thereby unavailable for decomposition by microbes now becomes available (Svensson et al. 1999; Christensen et al. 2004; Ström and Christensen 2007; Olefeldt et al. 2013). The disintegration of permafrost also causes overall wetter conditions as the soil becomes saturated in water. The combination of the high availability of organic carbon and waterlogged soils in turn leads to anaerobic conditions as microbes begin to decompose carbon and subsequently depleting all

available oxygen (Schelesinger and Bernhardt 2013). It is in anaerobic environments such as these that the process of CH_4 production, or methanogenesis, can take place (Schelesinger and Bernhardt 2013). Before methanogenesis occurs, however, there is a hierarchy in terms of oxidants that is used during the decomposition by microbes. This order is determined by the energy yield of the respective metabolic pathway and since microbes tend to go for the oxidant that will lead to the highest energy yield, oxygen (O_2) will be the first to be depleted through aerobic respiration, as described above. This is followed by anaerobic respiration of nitrate (NO^-_3), manganese (Mn^{4+}), iron (Fe^{3+}) and finally sulphate (SO_4^{2-}) (Schelesinger and Bernhardt 2013). Once all oxidants previously mentioned have been depleted and there is still organic material left to be decomposed (in combination with methanogenic substrates and microbes) methanogenesis takes place (Schelesinger and Bernhardt 2013).

Another condition for methanogenesis is the substrate availability. Here the vegetation plays a key role, as it directly influences the substrate availability through so called root exudates (Holzapfel-Pschorn 1986). In other words, these exudates are what is providing the methanogenic substrates which in turn are taken up by methanogenic bacteria in order to produce CH_4 (Holzapfel-Pschorn 1986). The exudates are released from the roots in the form of e.g., amino acids, carboxylic acids, and carbohydrates (Fischer et al. 2007).

The production of CH_4 can occur through two main pathways; acetoclastic or hydrogenotrophic (Kotsyurbenko et al. 2004; Olefeldt et al. 2013; Schelesinger and Bernhardt 2013). Acetoclastic methanogenesis has a higher energy yield and is therefore the first one to take place, given that the appropriate methanogenic microbial community and substrates are available (Kotsyurbenko et al. 2004). In this process acetate is split and CO_2 and CH_4 is produced as an end-product. When acetate is depleted or unavailable as a substrate hydrogenotrophic methanogenesis occurs. In this process CO_2 is reduced at the same time as H_2 is fermented, and CH_4 and H_2O is produced as a result (Kotsyurbenko et al. 2004; Schlesinger and Bernhardt 2013).

When CH_4 has been produced in the anoxic soils, there are three main pathways in which it can be transported into the atmosphere; diffusion through the water and waterlogged soils, ebullition and through the aerenchymateous tissue of plants (Figure 2) (Joabsson et al. 1999; Olefeldt et al. 2013; Schlesinger and Bernhardt 2013). Diffusion is the movement of CH_4 from the soil or water into the atmosphere (or the other way around) as a result of differences in concentrations between the soil or water and air (Olefeldt et al. 2013; Schlesinger and Bernhardt 2013). Ebullition is the transport of CH_4 through gas bubbles containing high concentrations of CH_4 through

the water body into the atmosphere (Olefeldt et al. 2013; Schlesinger and Bernhardt 2013). These bubbles form when there is a build-up of CH_4 to the point of which it exceeds the hydrostatic pressure of the surrounding water (Matson and Harriss 2009).

The final means of transportation for CH_4 is through the aerenchyma of stems and roots of certain sedges vegetation that are adapted to wetland ecosystems (Olefeldt et al. 2013; Schlesinger and Bernhardt 2013). These plants have the ability to transport O_2 down to their root system, which in turn allows methanotrophs, a group of methane consuming bacteria, to oxidise CH_4 into CO_2 through the process of methanotrophy. However, as the O_2 is transported down to the roots, the aerenchyma also allows CH_4 to escape in the other direction (Olefeldt et al. 2013; Schlesinger and Bernhardt 2013). This allows a portion of the CH_4 to move directly past the oxic peat layer, through the aerenchyma and directly into the atmosphere without being completely oxidized into CO_2 by methanotrophs (Holzapfel-Pschorn 1986; Joabsson et al. 1999; Ström et al. 2005; Olefeldt et al. 2013; Schlesinger and Bernhardt 2013).

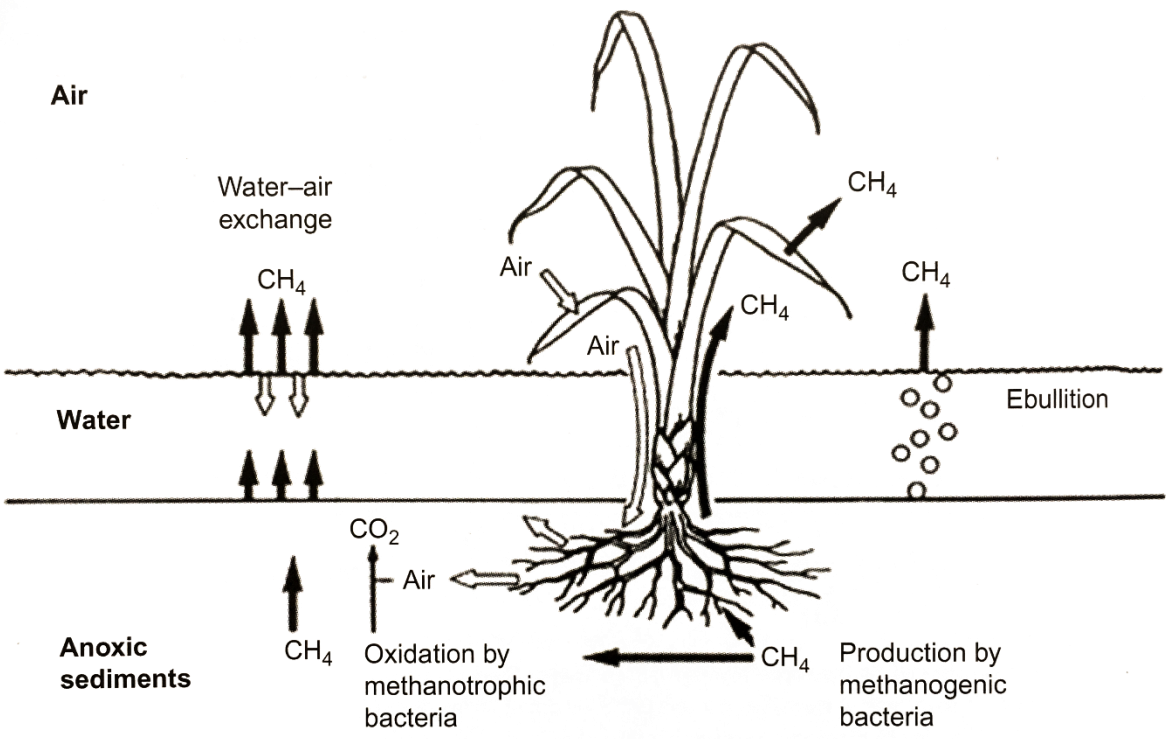

Figure 2. Scheme showing the process of CH_4 production, oxidation, and transport (diffusion, ebullition, through aerenchyma) (Figure from Schutz et al. 1991 in Schlesinger and Bernhardt 2013).

2.3.2. CO_2 exchange

In the terrestrial ecosystem carbon is taken up as CO_2 by plants and stored as biomass through the process of photosynthesis. This photosynthetic uptake of CO_2 is known as the gross primary production (GPP) (Schaefer et al. 2012; Schelesinger and Bernhardt 2013). As carbon is taken up by plants a portion is also released through autotrophic respiration (R_a) (Schaefer et al. 2012; Schelesinger and Bernhardt 2013). Furthermore, in aerobic environments, i.e., where O_2 is still available, aerobic heterotrophic respiration (R_h) occurs, where microbes use O_2 in the decomposition of organic material (Holzapfel-Pschorn 1986; Schelesinger and Bernhardt 2013). This pathway, as opposed to the anaerobic respiratory pathways described in the previous section, result in a complete degradation of the organic material into CO_2, through the R_h by microbes (Schelesinger and Bernhardt 2013). The total ecosystem respiration (R_{eco}) is consequently defined as the sum of autotrophic and heterotrophic respiration ($R_{eco} = R_a + R_h$) (Schaefer et al. 2012; Schelesinger and Bernhardt 2013). Finally, net ecosystem exchange (NEE) is the net release or uptake of CO_2 and is defined as the difference between R_{eco} and GPP (NEE = R_{eco} - GPP) (Schaefer et al. 2012; Schelesinger and Bernhardt 2013).

The uptake and release of CO_2 impacts the overall carbon storage in the ecosystem, which in turn influence the substrate availability. A higher CO_2 uptake leads to a greater biomass storage (GPP) and in turn R_a. A higher uptake of CO_2 may also stimulate root exudation and thereby providing substrates for microbes and increasing the R_h. Furthermore, a higher substrate availability may also stimulate methanogenesis (Holzapfel-Pschorn 1986; Schaefer et al. 2012; Schelesinger and Bernhardt 2013).

3. Materials and methods

3.1. Study area

All data used in this study was sampled in the subarctic permafrost region located around Abisko at 68°22’N, 19°03’E in northern Sweden (Figure 3). The Abisko area has an annual mean air temperature of approximately 0.5°C, an annual precipitation of approximately 332 mm and is located between 342-932 m above sea level (Callaghan et al. 2013). The sampling was performed in three different mires: Storflaket, Kursflaket and Katterjokk. These specific mires were chosen based on their state of permafrost degradation. Storflaket has a relative stable and intact permafrost, Kursflaket has slightly less permafrost and a deeper AL and Katterjokk has undergone a complete loss of permafrost.

Storflaket (68°20’51’’N, 18°57’55’’E) and Kursflaket (68°21’05’’N, 18°52’42’’E) are both peat plateaus underlain by discontinuous and sporadic permafrost. In the last decades, the AL has deepened at a rate of ca. 0.007 m/year in Storflaket and approximately 0.01 m/year in Kursflaket (Åkerman and Johansson 2008). Katterjokk (68°21’05’’N, 18°52’42’’E), however, is a smaller isolated bog with low palsas, with no traceable permafrost (Åkerman and Johansson 2008).

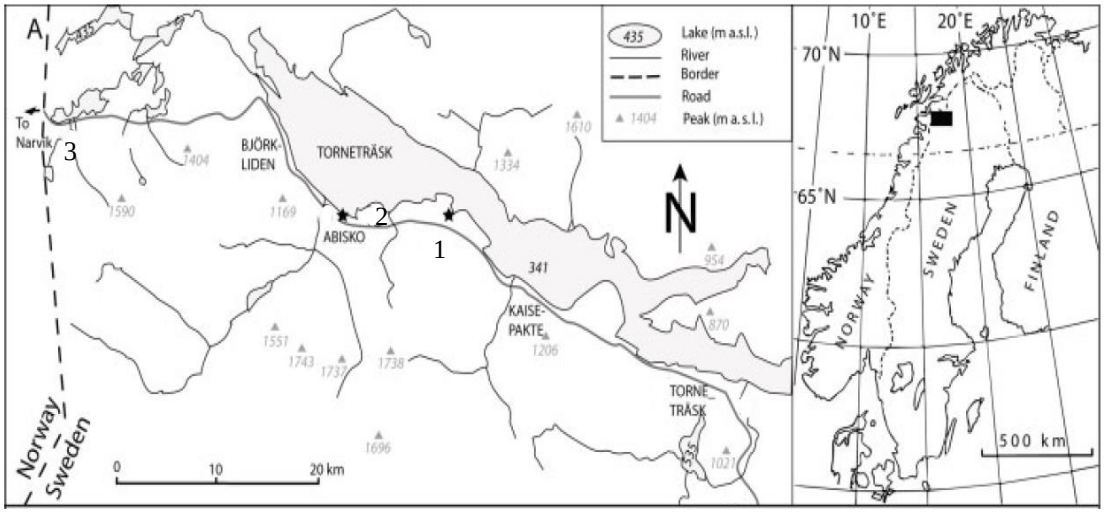

Figure 3. Map of study area and the locations of the three sites: Storflaket (1), Kursflaket (2) and Katterjokk (3). Left star shows the location Abisko Scientific Research Station and right star indicates the location of Stordalen (Figure from Knutsson 1980 in Åkerman and Johansson 2008).

The vegetation varied between the sites; however, all sites were dominated by different types of shrubs and sedges. The main shrub species throughout the three sites were *Andromeda polifolia, Betula nana, Empetrum nigrum.* The dominating species of sedges were mainly *Carex bigelowii, Carex flacca, Carex rostrata, Eriophorum angustifolium, Eriophorum vaginatum.* A complete description of the species composition at each site and plot can be found in Appendix A, Table S1- S3.

3.2. Data sets and measurements

All measurements were taken between 2019-07-18 and 2019-08-11 between approximately 10 am - 5 pm each day. A total of 16 plots were set up at Storflaket and Kursflaket and eight plots were set up at the Katterjokk site. At each plot five replicate measurements were taken of CO_2 and CH_4 concentrations (in dark and light conditions), WTD, AL depth, T_{air} (air temperature) and T_{soil} (soil temperature) in order to gather the variability within each plot. Additionally, the dominant vegetation types were noted for each plot (Appendix A, Table S1- S3).

The measurements of the CO_2 and CH_4 concentrations were taken using the closed-chamber method i.e., there was no inflow or outflow of air from the chamber or atmosphere (Falk et al. 2014; Falk et al. 2015). Permanent stainless-steel bases were installed at each plot at all three sites. The permanent bases were installed in the end of June, with measurements starting in the beginning of July. During the measurements transparent plexiglass chambers were placed on top of the base. The chambers used had a height of 315 mm and the permanent bases had a diameter of 300 mm and were installed 300 mm into the ground. In order to ensure that the air inside the chambers was properly mixed during the measurements, a fan was installed inside each chamber. The chambers were in turn connected to a portable Fourier transform infrared (FTIR) spectrometer (Gasmet Dx 40-30, Gasmet Technologies Oy, Finland) which measured the concentrations of the gases on the above-mentioned days. Measurements of CO_2 and CH_4 concentrations were taken in both light conditions and in dark conditions for each plot and replicate measurement every two seconds. The dark conditions were achieved by covering the chamber with a non-transparent cover directly after the light measurements was taken. The measurements of CO_2 in light conditions represents the NEE and the same measurements during dark conditions represents R_{eco}. The variable GPP was then calculated by subtracting the NEE from R_{eco} ($GPP = R_{eco} - NEE$).

In addition to the measurements of gas concentrations, measurements of WTD (cm below surface), AL depth (cm below surface), T_{air} and T_{soil} were also taken at the immediate vicinity of each plot and replicate measurement. Measurements of T_{soil} were taken using a handheld electrode and temperature sensor of the model pH 110 (VWR, part of Avantor) and AL depth was measured using a 1 m probe. Measurements of WTD were taken by first installing a PVC-pipe with holes in the soil, in order to let water enter and thereby creating an equilibrium with the water table. Next, the position of the water table within the pipe was measured in relation to the vegetation surface.

3.3. Data treatment

3.3.1 Flux calculations

In order to calculate the carbon fluxes a linear regression ($y = kx + m$) was performed on the CO_2 and CH_4 measurements in MS Excel using Eq. 2, derived from the Ideal gas law (Eq. 1):

$$PV = nRT \rightarrow n = \frac{PV}{RT} \qquad \textbf{Eq. 1}$$

, where n is the number of moles, P is pressure of the gas (Pa) at sea level, V is the volume of the gas in the chamber (m^3) R is the ideal gas constant ((8.314 m^3 Pa)/(mol·K)) and T is the temperature of the gas (K).

$$Flux\ (mg\ m^{-2}h^{-1}) = \frac{k\ \cdot C_{volume} \cdot M \cdot (P \cdot 100) \cdot 1000 \cdot 60}{1000000 \cdot R \cdot (T_{air} + 273.15) \cdot\ C_{area}} \qquad \textbf{Eq. 2}$$

, where k is the slope of the linear regression describing the change in CH_4 or CO_2 concentration over time (ppm/min), C_{volume} is the area·height of the gas chamber, M is the molar mass of CH_4 or CO_2 (g), P is the atmospheric air pressure (hPa) at the respective site and T_{air} is the air temperature at the respective site (°C).

The gas concentrations were recorded using 1-second intervals. For the linear regression of CO_2, the original 1-second interval measurements were used. However, for the regression of CH_4 the gas concentrations were recalculated into 30-second averages in order to compensate for a lower resolution in the CH_4 measurements at low fluxes. When calculating the fluxes using linear regression and Eq. 2, the regressions were accompanied by an r^2-value. In certain cases, the r^2-value was quite low, and in these cases, they were almost always accompanied by low fluxes. The low fluxes could simply be an indication of a dry plot. However, since these fluxes were so low, the linear regression was quite hard to do, as no linear relationship could be found. In order to determine whether or not these fluxes were usable, calculations of RMSE were conducted on a very small subset of the low fluxes. The RMSE shows the magnitude of error and would thereby give an indication of the quality of the measurements. The calculations showed the low fluxes with low r^2-value also had a low RMSE ($\leq 2\%$) and were therefore deemed usable for this study.

Next the calculated CH_4 or CO_2 fluxes for each plot and replicate measurement were carefully looked over in order to find inaccurate values based on specific criteria. In this process dark CO_2 fluxes that had a negative value were set to zero, since these cannot have values below zero. Furthermore, negative measurements of CH_4 light were discarded since these values are not possible and are most likely a result of instrument malfunction during the sampling.

Finally, for each variable, the five replicate measurements at each plot were used to calculate one mean value that was used for statistical analyses.

3.3.2 Statistical analysis

All plotting and statistical analysis was done in R (RStudio version 1.4.1106) using the following packages: ggplot2 (Wickham 2016), dplyr (Wickham et al. 2021), agricolae (de Mendiburu 2020) and ggpmisc (Aphalo 2021), Metrics (Hamner and Frasco 2018), corrplot (Wei and Simko 2017), Hmisc (Harrell 2021) and ggpubr (Kassambara 2020).

In order to test the difference between the three sites (Katterjokk, Kursflaket and Storflaket), a Shapiro-Wilk normality test was first performed on each of the carbon fluxes (CH_4, Reco, GPP and NEE) to check whether or not the datasets were normally distributed. The Shapiro-Wilk test indicated that not all parameters were normally distributed, thereby the assumptions for a following one-way ANOVA were not met and the Kruskal-Wallis rank sum test was instead chosen to test the significance between the three sites. If a significant difference between the sites were indicated by the Kruskal-Wallis test, a post-hoc pair-wise Wilcoxon test was followed in order to determine between which specific sites the significant difference lay.

For testing the difference in carbon fluxes between wet and dry plots the WTD measurements was used to divide all plots into two groups: “wet plots” and “dry plots”. Wet plots were defined as plots with a measurable water table, i.e., WTD < 50 cm (cm below the surface) and dry plots were defined as plots with a WTD ≥ 50 cm (cm below the surface). The threshold of 50 cm was chosen because this was the maximum depth of which the water table could be measured, as the length of the pipe used in the measurements was 50 cm and could therefore not go any deeper. Next, an unpaired two-samples Wilcoxon test was performed to determine the level of significance between the wet and dry plots.

Correlation matrices were generated using the corrplot-package created by Wei and Simko (2017) to get an overview of what parameters correlated and by what magnitude. Each correlation (Pearson correlation coefficient) was then tested for significance using the Hmisc package (Frank 2021). If a parameter had no variance i.e., same value for each data point throughout each site, such as for the AL depth in Katterjokk, these were replaced to avoid a standard deviation of zero and consequently division by zero when calculating the correlation coefficients. The Katterjokk-site had an AL depth below 100 cm (the maximum length of the probe used to measure the AL). In order to create variance for the AL depth in Katterjokk, 8 random uniformly distributed numbers were generated between 100 cm-100.1 cm. These values were chosen to keep the 8 random numbers as close to the true value (100 cm) as possible while still creating a variance. They were generated randomly to avoid creating any unwanted trends that are not

actually there. The randomly generated values for AL depth replaced the original values for Katterjokk in the statistical analysis.

4. Results

4.1. Carbon fluxes between sites

4.1.1. CH_4 fluxes

The carbon fluxes for each site are illustrated in Figure 4. Overall, the fluxes of CH_4 ranged between a median of approximately 0 and 5 mg CH_4 m^{-2} h^{-1}. When visually examining the results, it was evident that Katterjokk had substantially a higher median CH_4 flux (ca. 5 mg CH_4 m^{-2} h^{-1}) compared to Kursflaket (ca. 0.6 mg CH_4 m^{-2} h^{-1}) and Storflaket (ca. 0 mg CH_4 m^{-2} h^{-1}), which had a quite similar median CH_4 flux. A Kruskal-Wallis test showed that there was a significant difference in CH_4 flux between the sites (p-value = 0.019). A post-hoc pair-wise Wilcoxon test confirmed that a significant difference lied between Katterjokk and Storflaket (p-value = 0.028) and Katterjokk and Kursflaket (p-value = 0.021). Moreover, there was no significant difference between Storflaket and Kursflaket (p-value = 0.585).

4.1.2. CO_2 fluxes

The R_{eco} was higher for Kursflaket with a median flux of approximately 425 mg CO_2 m^{-2} h^{-1}, compared to Katterjokk (ca. 300 mg CO_2 m^{-2} h^{-1}) and Storflaket (ca. 325 mg CO_2 m^{-2} h^{-1}), which had quite similar median fluxes. The Kruskal-Wallis test showed that there were significant differences between the sites (p-value = 0.012). The following post-hoc Wilcoxon test showed significant differences between Kursflaket and Katterjokk (p-value = 0.029) and Kursflaket and Storflaket (p-value = 0.029). There was no significant difference between Storflaket and Katterjokk (p-value = 0.569).

GPP was highest for Katterjokk (ca. -470 mg CO_2 m^{-2} h^{-1}) and Kursflaket (ca. -435 mg CO_2 m^{-2} h^{-1}), which had quite similar values, compared to Storflaket with the lowest median flux at approximately -375 mg CO_2 m^{-2} h^{-1}. The Kruskal-Wallis test showed that there were no significant differences between the sites (p-value = 0.201).

The NEE was highest in Katterjokk with a median flux of around -150 mg CO_2 m^{-2} h^{-1}, compared to the medians of Kursflaket (ca. 0 mg CO_2 m^{-2} h^{-1}) and Storflaket (ca. -50 mg CO_2 m^{-2} h^{-1}). The Kruskal-Wallis test showed that there were significant differences between the sites (p-value $\leq$ 0.001) The following post-hoc Wilcoxon test showed that

the significance lied between Kursflaket and Katterjokk (p-value ≤ 0.001) and between Storflaket and Katterjokk (p-value = 0.009). There was no significant difference between Kursflaket and Storflaket (p-value = 0.119).

Overall, all sites had negative NEE, which indicate that there was a net uptake of CO_2 in all three sites (Figure 4). There was, however, significant differences in the level of uptake between the sites. The NEE was significantly higher at Katterjokk compared to Storflaket and Kursflaket, which both had quite similar NEE with median values slightly below the zero mark. Furthermore, the GPP is a direct result of the R_{eco} (CO_2 release) and NEE (CO_2 uptake), as these are used for estimating the GPP. Katterjokk had a high NEE i.e., a high uptake of CO_2 in combination with a low R_{eco} (CO_2 release), compared to the other sites. Therefore, the GPP was quite high at this site, resulting in an uptake. Furthermore, Kursflaket had a NEE close to zero in combination with a quite high R_{eco}, which in turn also resulted in a GPP close to what was seen at Katterjokk (Figure 4). The same pattern was also seen for Storflaket where a similar GPP was observed (Figure 4).

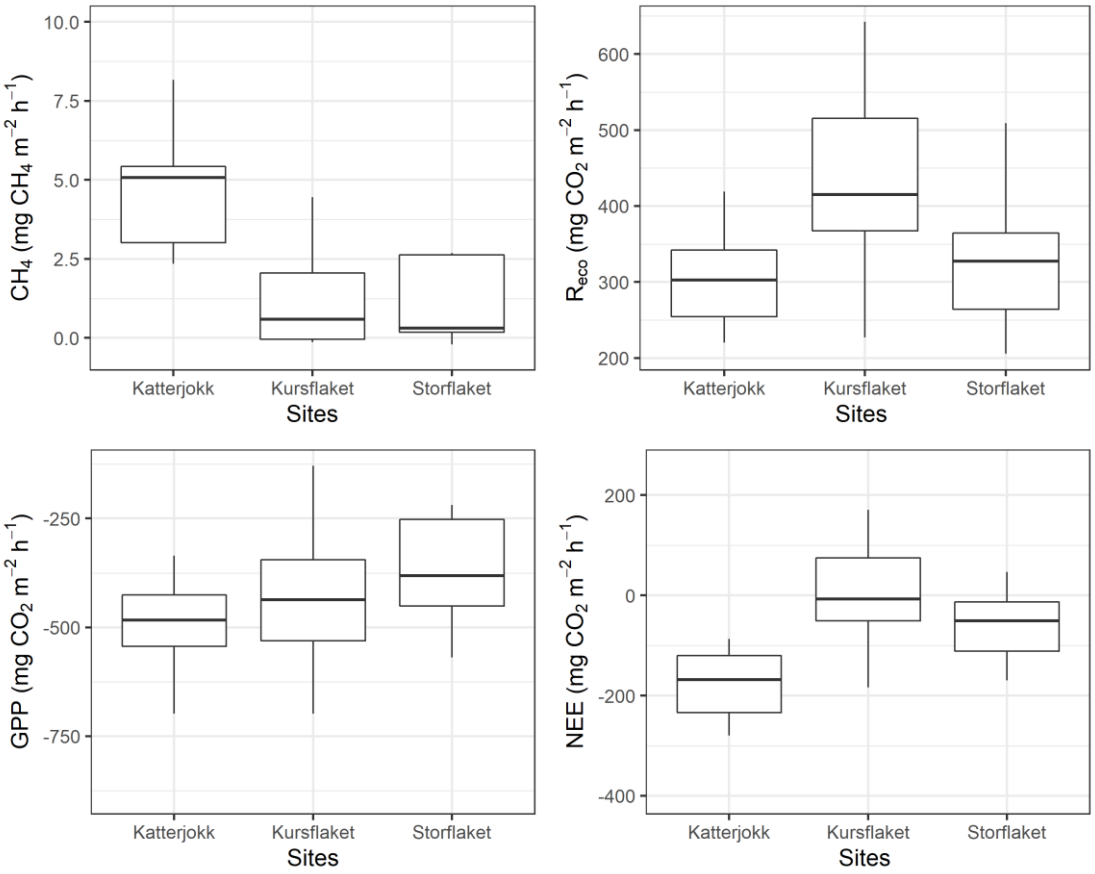

Figure 4. Boxplots showing the median, interquartile range and maximum and minimum of CH_4 in mg CH_4 m^{-2} h^{-1} and R_{eco}, GPP and NEE in mg CO_2 m^{-2} h^{-1} for each site: Katterjokk (n = 8), Kursflaket (n = 16) and Storflaket (n = 16).

4.2. Carbon fluxes within sites

4.2.1. Katterjokk

Figure 5 shows the variation in carbon flux for each plot within Katterjokk. A substantial difference between the plots for all fluxes was observed. For fluxes of CH_4, plots 1-3 and 6 had a slightly lower flux with a median around 3-4 mg CH_4 m^{-2} h^{-1}, whereas plots 4-5 and 7-8 had a median flux of approximately 5 mg CH_4 m^{-2} h^{-1}.

The highest flux for R_{eco} was observed in plots 2 and 7 with approximately a median flux of 470 mg CO_2 m^{-2} h^{-1}, this was then followed by plots 3, 5 and 8 which had intermediate fluxes of around 300-350 mg CO_2 m^{-2} h^{-1}. Plots 1, 4 and 6 had the lowest R_{eco} of around 200-250 mg CO_2 m^{-2} h^{-1}.

The GPP was highest at plot 7 with a median flux of approximately -750 mg CO_2 m^{-2} h^{-1} followed by plot 8 and 3, with a median flux of around -550 mg CO_2 m^{-2} h^{-1}. Plots 1 and 4-6 had the lowest median GPP of around -300 and -400 mg CO_2 m^{-2} h^{-1}.

Fluxes of NEE were highest at plots 3 and 7, with a median ranging around ca. -275 mg CO_2 m^{-2} h^{-1} followed by plots 5-6 and 8 with median fluxes around -200 mg CO_2 m^{-2} h^{-1}. Plots 1-2 and 4 had the lowest NEE around ca. -150 mg CO_2 m^{-2} h^{-1}.

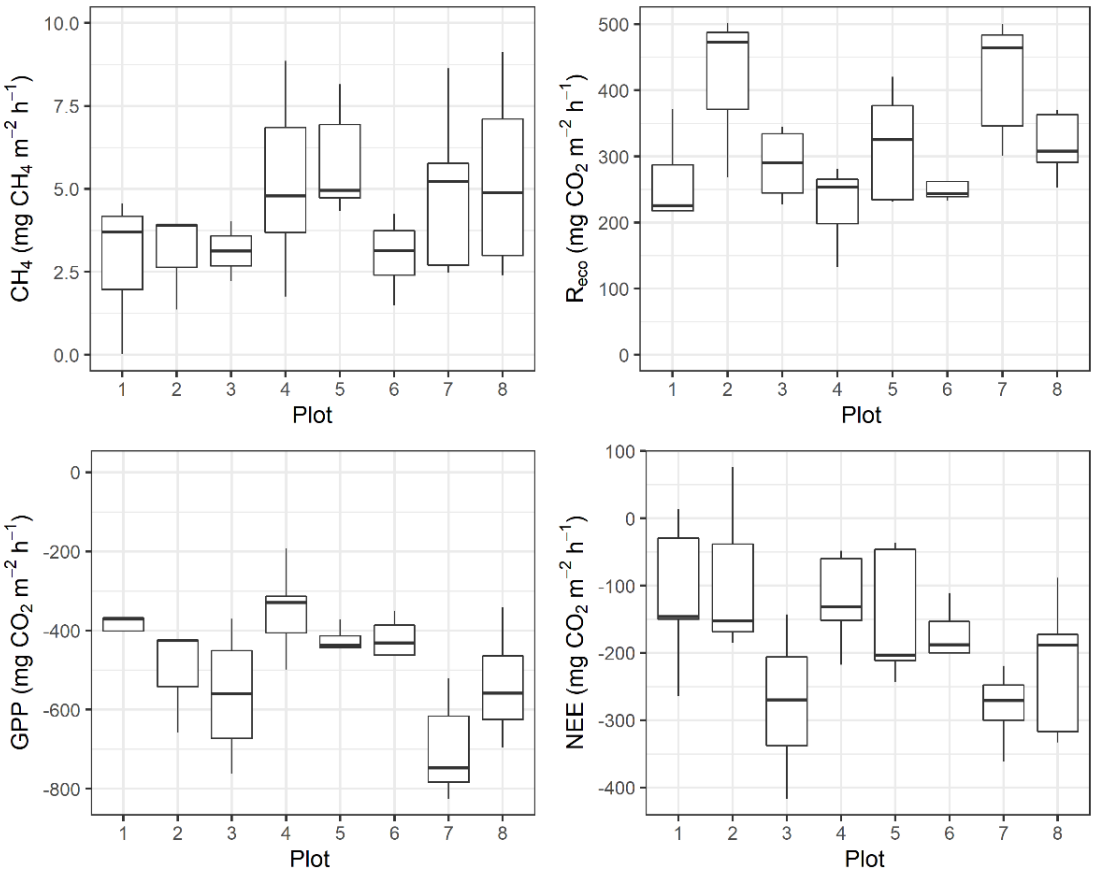

Figure 5. Boxplots showing the median, interquartile range and maximum and minimum of CH_4 in mg CH_4 m^{-2} h^{-1} and R_{eco}, GPP and NEE in mg CO_2 m^{-2} h^{-1} for each plot in Katterjokk.

4.2.2. Kursflaket

Figure 6 shows the variation in carbon fluxes for each plot within Kursflaket. This site also exhibited large differences between the plots for all fluxes. For fluxes of CH_4, plots 1-6, 8 and 15-16 had quite low median fluxes of around 0-1 mg CH_4 m^{-2} h^{-1}. Plots 9, 11-12 had intermediate fluxes with medians ranging between 1-1.5 mg CH_4 m^{-2} h^{-1}. Plots 7, 10 and 13-14 had notably higher fluxes compared to the other plots, with medians ranging between ca. 3-5.5 mg CH_4 m^{-2} h^{-1}. Out of these, plot 14 had the highest median flux.

The lowest fluxes of R_{eco} were observed in plots 2-7, 12-13 and 16, where the median flux ranged between approximately 200 and 450 mg CO_2 m^{-2} h^{-1}. Out of these plots 6-7 had the lowest median fluxes. The highest fluxes were observed in plots 1, 8-11 and 14-15 with a range of ca. 450 and 550 mg CO_2 m^{-2} h^{-1}.

The GPP was lowest for plots 1-3 and 5-8 and 16 ranging between a median of approximately -150 and -400 mg CO_2 m^{-2} h^{-1}. Out of these, plots 6-7 had the lowest

GPP. Remaining plots had a higher GPP with a range of ca. -500 and -700 mg CO_2 m^{-2} h^{-1}.

The NEE for plots 1-2 and 5-9 had median fluxes ranging between 0-200 mg CO_2 m^{-2} h^{-1}, whereas remaining plots had negative median fluxes ranging between approximately 0 and -200 mg CO_2 m^{-2} h^{-1}.

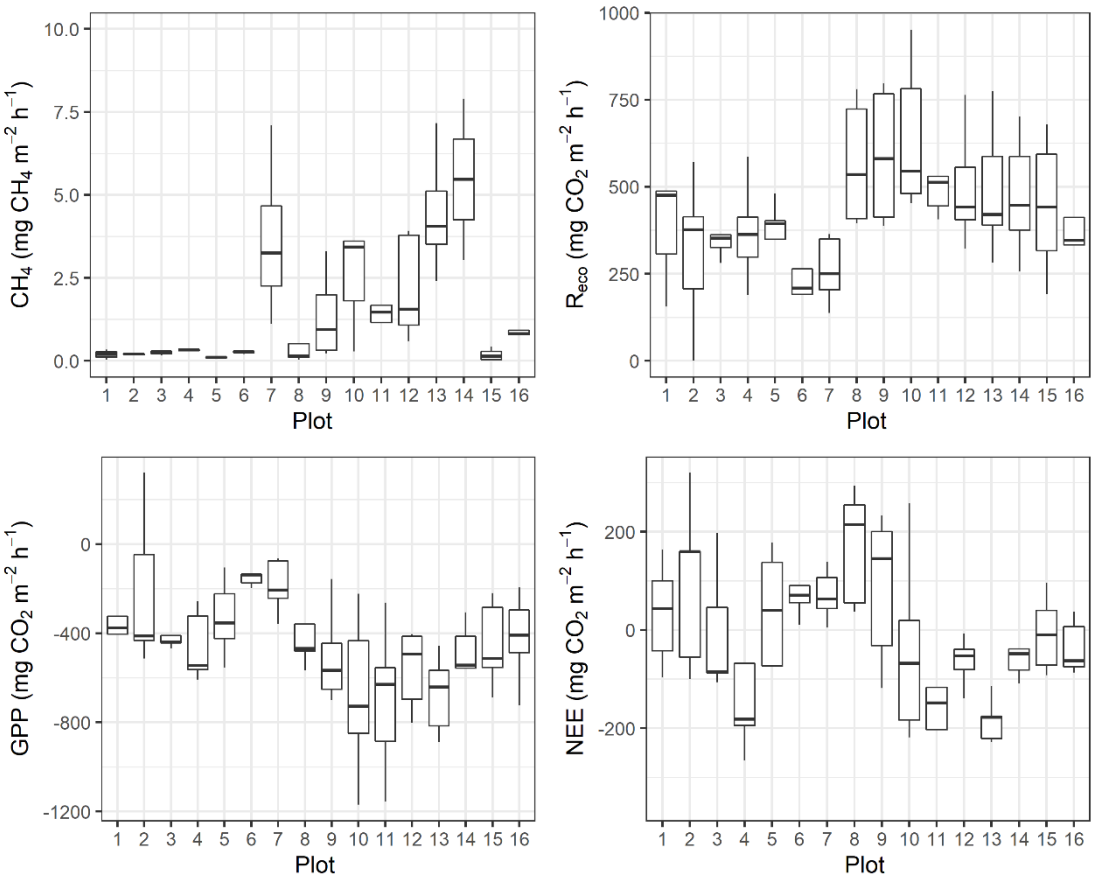

Figure 6. Boxplots showing the median, interquartile range and maximum and minimum of CH_4 in mg CH_4 m^{-2} h^{-1} and R_{eco}, GPP and NEE in mg CO_2 m^{-2} h^{-1} for each plot in Kursflaket.

4.2.3. Storflaket

Figure 7 shows the variation in carbon fluxes for each plot within Storflaket. Notable differences between the plots for all fluxes were observed. Fluxes of CH_4 were generally quite low for plots 1-12, with a median range of ca. 0-2.5 mg CH_4 m^{-2} h^{-1}, remaining plots had substantially higher median fluxes ranging from ca. 5 mg CH_4 m^{-2} h^{-1} up to 6.5 mg CH_4 m^{-2} h^{-1}.

The R_{eco} did not have as big spread in fluxes as was observed at the other sites (Figure 5 and 6). All fluxes ranged between approximately 160 and 450 mg CO_2 m^{-2} h^{-1},

however most plots had a median around 300 mg CO_2 m^{-2} h^{-1}, apart from plot 13 which had a median flux of ca 460 mg CO_2 m^{-2} h^{-1}.

Substantial variations were observed in the GPP. Plots 1, 8-10 and 14-16 had the lowest fluxes ranging between -300 and -125 mg CO_2 m^{-2} h^{-1}. Furthermore, plots 2-7 and 11-12 had slightly higher fluxes with a range of -350 and 600 mg CO_2 m^{-2} h^{-1} and plot 13 had the highest GPP of ca. -1000 mg CO_2 m^{-2} h^{-1}.

The NEE in plots 2-7 and 9-16 ranged between ca 0 and -125 mg CO_2 m^{-2} h^{-1}, with the exception of plot 13 which had a median flux of approximately -500 mg CO_2 m^{-2} h^{-1}. Remaining plots ranged between 0-250 mg CO_2 m^{-2} h^{-1}, with the highest flux of ca 250 mg CO_2 m^{-2} h^{-1} seen in plot 1.

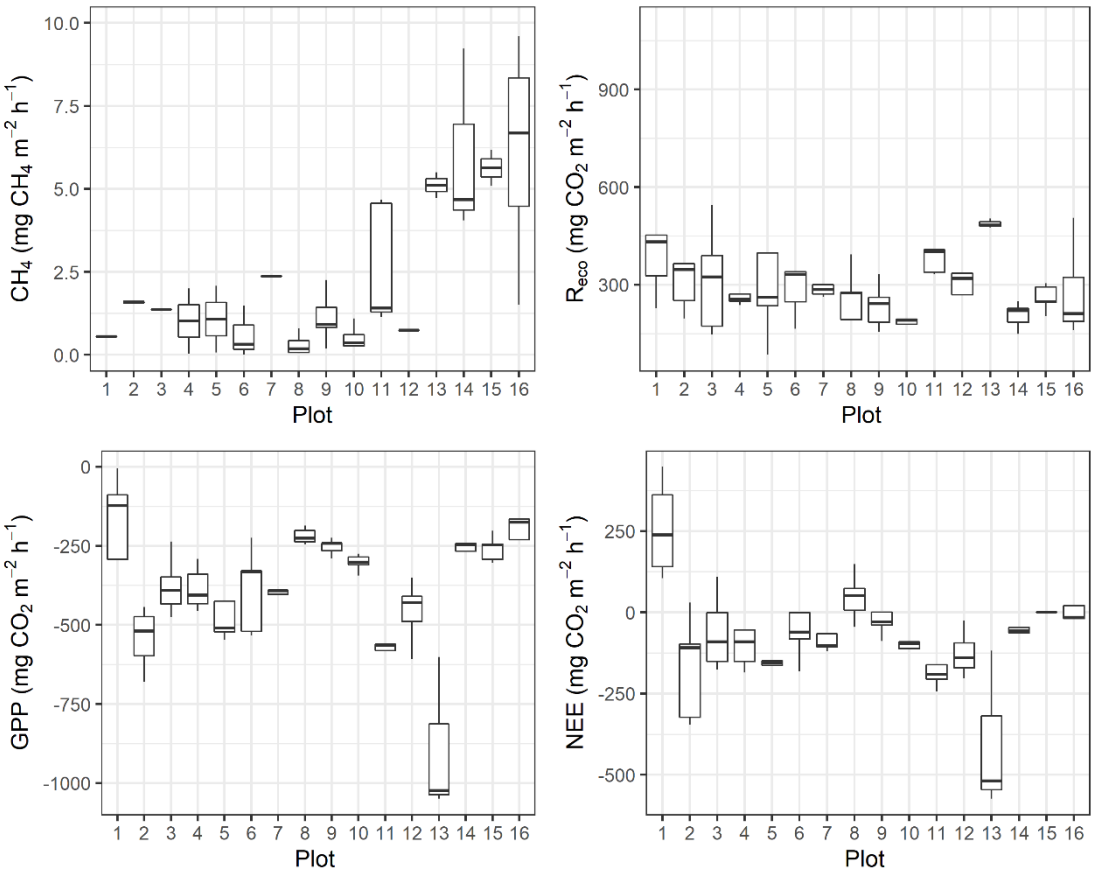

Figure 7. Boxplots showing the median, interquartile range and maximum and minimum of CH_4 in mg CH_4 m^{-2} h^{-1} and R_{eco}, GPP and NEE in mg CO_2 m^{-2} h^{-1} for each plot in Storflaket.

4.3. Drivers of the carbon fluxes

The linear relationships between all the variables are shown in Figure 8. Overall, there were some quite strong correlations between GPP and R_{eco} and GPP and NEE in all sites, as well as in each site individually, as both R_{eco} and NEE are used to derive the

GPP. Furthermore, when looking at all sites together (Figure 8, A) the strongest correlation was seen for WTD vs. AL depth (r-value = -0.82, p-value ≤ 0.0001), WTD vs. CH_4 flux (r-value = -0.71, p-value ≤ 0.0001) and CH_4 flux vs. AL depth (r-value = 0.6, p-value = 0.002).

Katterjokk (Figure 8, B) exhibited quite weak correlations between WTD vs. AL depth (r-value = -0.35, p-value = 0.191) and WTD vs. CH_4 flux (r-value = 0.23, p-value = 0.133) and an intermediate correlation for CH_4 flux vs. AL depth (r-value = -0.5, p-value = 0.034). Kursflaket (Figure 8, C) on the other hand showed a strong correlation between WTD vs. AL depth (r-value = -0.92, p-value ≤ 0.0001) with an intermediate correlation between WTD vs. CH_4 flux (r-value = -0.57, p-value ≤ 0.001) and CH_4 flux vs. AL depth (r-value = -0.57, p-value = 0.009). Finally, Storflaket (Figure 8, D) exhibited strong correlations between WTD vs. AL depth (r-value = -0.73, p-value = ≤ 0.001) and WTD vs. CH_4 flux (r-value = -0.9, p-value ≤ 0.0001) and an intermediate correlation for CH_4 flux vs. AL depth (r-value = 0.62, p-value = 0.004).

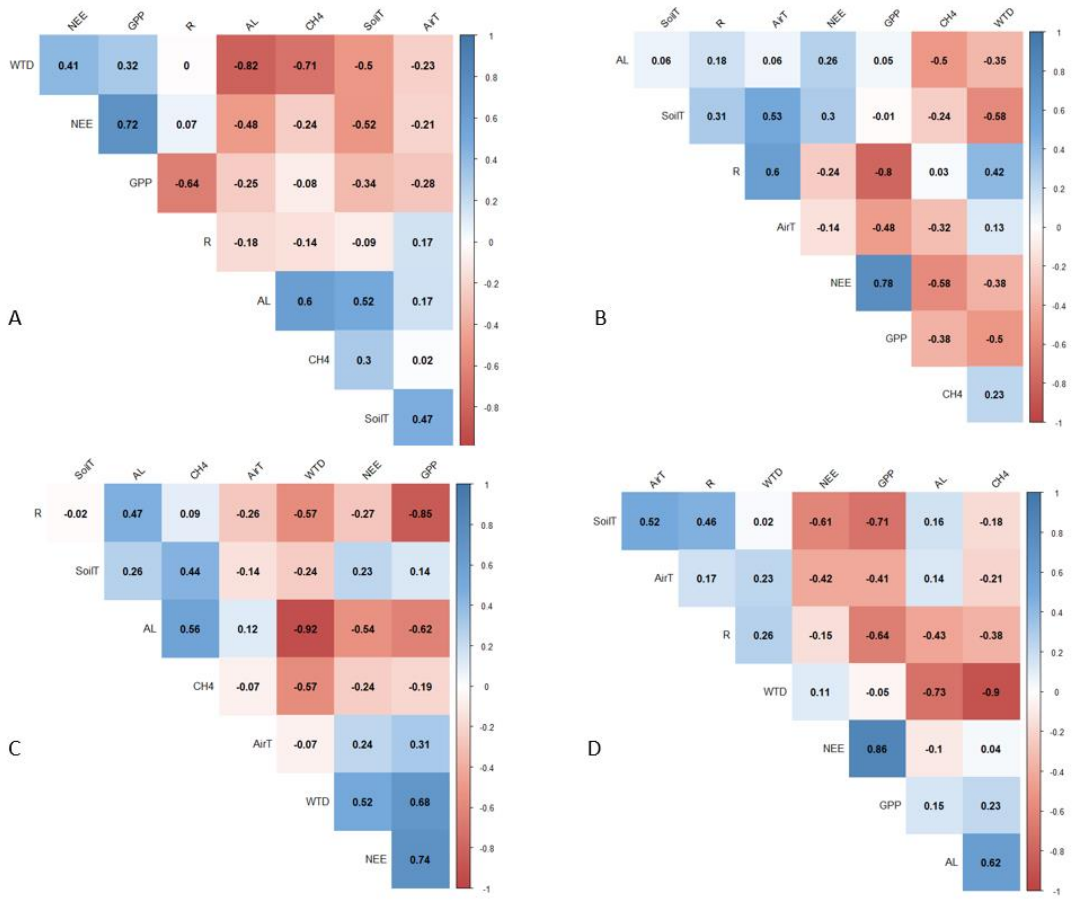

Figure 8. Correlation matrices showing the Pearson correlation coefficients (r-value) for all parameters against each other for each site and all sites together. All sites (n = 40) (A), Katterjokk (n = 8) (B), Kursflaket (n = 16) (C) and Storflaket (n = 16) (D).

4.4. Wet vs. dry plots

Figure 9 shows the variation in carbon fluxes for wet and dry plots. Fluxes of CH_4 were observed to be substantially higher at wet plots, compared to dry plots. The wet plots had a median CH_4 flux of ca. 3 mg CH_4 m^{-2} h^{-1}, as well as a larger range (0 to 10 mg CH_4 m^{-2} h^{-1}), whereas the dry plots had a median flux of 0 mg CH_4 m^{-2} h^{-1}. A two-sampled Wilcoxon test confirmed that there was a significant difference in CH_4 flux between the wet and dry plots (p-value $\leq$ 0.0001).

The R_{eco} at the wet and dry plots were quite similar with a median flux around 375 mg CO_2 m^{-2} h^{-1}, however the ranges differed quite a lot. Wet plots ranged between approximately 200 and 625 mg CO_2 m^{-2} h^{-1}, whereas the dry plots had a smaller range (ca. 250 to 450 mg CO_2 m^{-2} h^{-1}). A two-sampled Wilcoxon test showed no significant difference in R_{eco} between the wet and dry plots (p-value = 0.533).

The GPP was quite similar between wet and dry plots. Dry plots had a median GPP of ca. -400 mg CO_2 m^{-2} h^{-1} and the wet spots had a slightly higher median flux of -500 mg CO_2 m^{-2} h^{-1}. The range was higher for the wet plots (-900 to -200 mg CO_2 m^{-2} h^{-1}), compared to the dry plots (-600 to -100 mg CO_2 m^{-2} h^{-1}). The two-sampled Wilcoxon test showed that there was a significant difference in GPP between the wet and dry plots (p-value = 0.045).

The NEE was also quite similar between wet and dry plots, as they both had a median flux around -75 mg CO_2 m^{-2} h^{-1}. The range was higher for the wet plots (-300 to 200 mg CO_2 m^{-2} h^{-1}), compared to the dry plots (-200 to 100 mg CO_2 m^{-2} h^{-1}). The two-sampled Wilcoxon test showed that there was no significant difference in NEE between the wet and dry plots (p-value = 0.149).

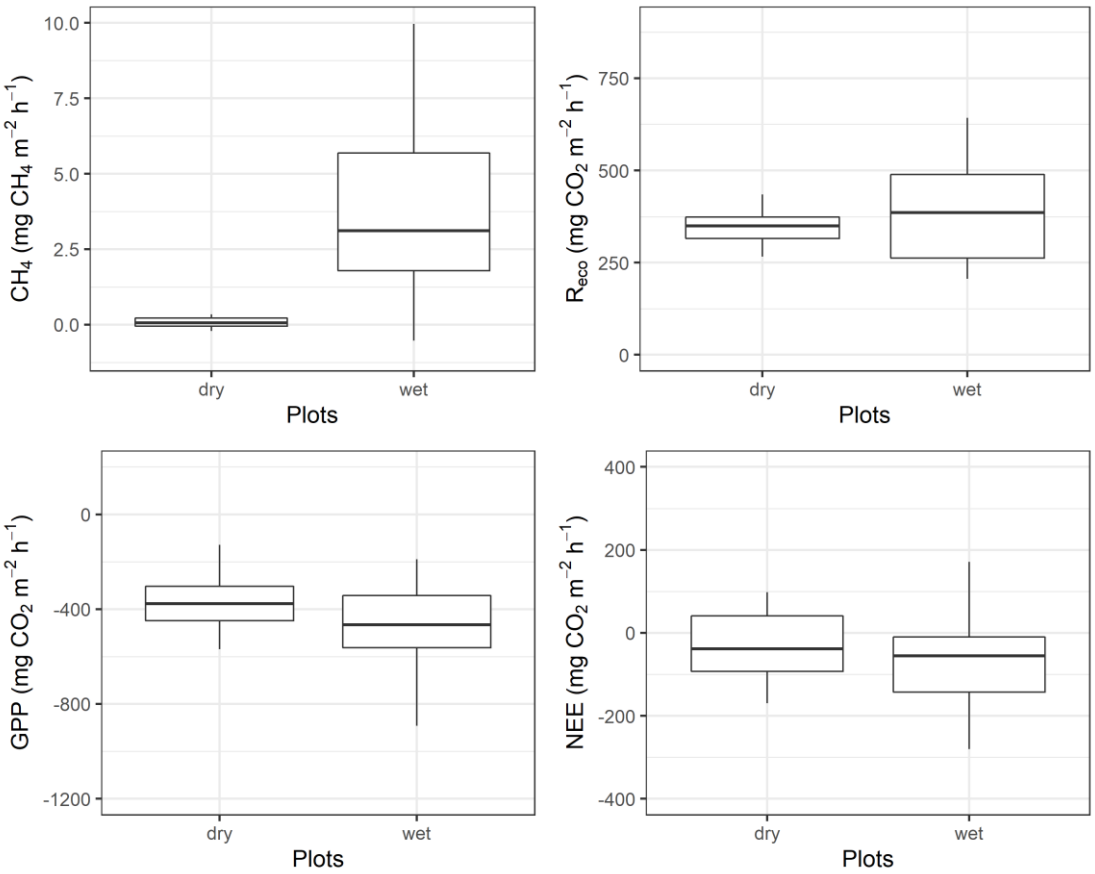

Figure 9. Boxplots showing the median, interquartile range and maximum and minimum of CH_4 in mg CH_4 m^{-2} h^{-1} and NEE, R and GPP in mg CO_2 m^{-2} h^{-1} for wet (n = 23) and dry plots (n = 17).

4.5. Environmental variables

An overview of each environmental variable at the three sites is provided in Table 1. The mean T_{soil} (12.20 ^{o}C) and T_{air} (18.72 ^{o}C) and WTD (8.22 cm below the surface) were highest at Katterjokk, followed by Kursflaket (T_{soil} = 8.63^{o}C, T_{air} = 18.37^{o}C and WTD= 32.73 cm below the surface) and Storflaket (T_{soil} = 8.51^{o}C, T_{air} = 17.34^{o}C and WTD= 37.99 cm below the surface) which had quite similar values. Katterjokk had no permafrost, Storflaket had the deepest mean AL (75.41 cm below the surface), followed by Kursflaket (65.17 cm below the surface).

Table 1. Summary table showing the mean, median, maximum, and minimum of the measured environmental parameters for each site (Storflaket, Kursflaket and Katterjokk); T_{soil} and T_{air} in degrees Celsius, WTD and AL depth in cm below surface.

	T_{soil}	**T_{air}**	**WTD**	**AL**
Storflaket				
Mean	8.51	17.34	37.99	75.41
Median	8.00	17.10	>50	77.50
Max	13.40	23.10	>50	>100
Min	6.40	11.80	3.00	40.00
Kursflaket				
Mean	8.63	18.37	32.73	65.17
Median	8.60	18.10	31.00	55.00
Max	12.30	26.30	>50	>100
Min	-9.00	12.80	6.00	40.00
Katterjokk				
Mean	12.20	18.72	8.22	>100
Median	12.10	19.90	8.15	>100
Max	14.10	23.60	16.00	>100
Min	10.90	12.30	-1.00	>100

5. Discussion

5.1. CH_4 fluxes

The CH_4 fluxes seen in Katterjokk are significantly higher than in Kursflaket and Storflaket (Figure 4). This is also evident when looking at the individual plots of CH_4 at the different sites (Figure 5-7). In these cases, Katterjokk has quite high fluxes throughout all plots (Figure 5), whereas in Storflaket and Kursflaket the fluxes of CH_4 vary across the plots, with some of them having very low or no flux and others having intermediate to high fluxes (Figure 6-7). Katterjokk is the only site out of the three that has experienced a complete loss of permafrost. This site consequently also has the deepest AL and highest WTD (Table 1). These factors combined could be an important aspect as to why the CH_4 fluxes are higher at this site. An increase in water table leads to more anoxic conditions and subsequently CH_4 production and emission (Ström and Christensen 2007). Wetter sites typically also have a higher proportion of aerenchymateous vegetation, such as *Carex rostrata* which is abundant at Katterjokk (Appendix A, Table S1) (Rydin et al. 1999). Aerenchymateous vegetation are able to facilitate the transport of CH_4 from the roots directly to the atmosphere and thereby increase the fluxes at that particular site (Holzapfel-Pschorn 1986; Joabsson et al. 1999; Christensen et al. 2004; Malmer et al. 2005; Ström et al. 2005; Olefeldt et al. 2013; Schlesinger and Bernhardt 2013). In line with the findings in this study, similar relationships between CH_4 flux and AL depth and WTD respectively has been identified in numerous other studies (Johansson et al. 2006; Ström and Christensen 2007; Natali et al. 2015).

Another aspect as to why Katterjokk has significantly higher emissions of CH_4 could be related to the fact that this site has been permafrost free for approximately a decade (Christensen et al. 2004; Åkerman and Johansson 2008). For methanogenesis to occur, apart from requiring the right environment, the right substrates (e.g., acetate) and microbial community also need to be present. The substrates used for methanogenesis such as acetate, however, are produced separately by other microbes in oxic environments and later "trickled down" to the anoxic zone (Schelesinger and Bernhardt 2013; Dean et al. 2018). This production and transport of substrates may take a bit of time, thereby creating a time lag. Therefore, sites that have been disintegrating for a long time, or better yet, undergone a complete disintegration of permafrost, such as Katterjokk, may not have this delay, as substrates have been produced over a long time. Therefore, it might be speculated that methanogenic substrates may not be as limited in Katterjokk as in sites where permafrost disintegration is less advanced, such as Kursflaket and Storflaket.

The plots with the highest CH_4 fluxes in Kursflaket are dominated by a mixture of sedges such as *C. bigelowii, Carex chordorrhiza, E. angustifolium* and shrubs such as *A. polifolia, B. nana, E. nigrum* and *Rubus chamaemorus* (Appendix A, Table S2). Plots 13 and 14 have the highest CH_4 flux in Kursflaket and at these plots *C. bigelowii* and *E. angustifolium* are the dominating sedges (Appendix A, Table S2). Vegetation such as these, and *E. angustifolium* in particular, are typically associated with wet minerotrophic conditions (i.e., nutrient rich and low-lying areas) (Svensson et al. 1999). Additionally, *E. angustifolium* also have aerenchymateous tissue that enables gas exchange between the root system and the atmosphere (Holzapfel-Pschorn 1986; Joabsson et al. 1999; Ström et al. 2005; Olefeldt et al. 2013; Schlesinger and Bernhardt 2013).

Although Kursflaket still has permafrost in most plots, plots 13 and 14, however, are the only plots that has an AL < 1 m (apart from plot 15 which has an AL <1 m but a low flux). These two plots consequently also have the highest WTD. These factors may partly explain why these plots have a vegetation that is typically associated with wet sites with no permafrost, such as Katterjokk, and has the highest CH_4 flux at the site. An interesting observation here is plot 15. This plot also has an AL < 1 m as well as a high WTD, similar to plots 13-14, but has a substantially lower CH_4 flux. This could be explained by the vegetation composition at this plot. Although this plot also consists of both the shrub species *A. polifolia* and the sedge *C. bigelowii,* it lacks the aerenchymateous *E. angustifolium* and instead has *C. chordorrhiza. E. angustifolium* is a larger sedge compared to *C. chordorrhiza* and therefore may have larger and more aerenchymateous tissue and consequently may be able to transport more CH_4 (Joabsson and Christensen 2001). Many studies have emphasized the importance of plant mediated CH_4 transport and how they may be an important control on CH_4 fluxes, thereby making the species composition at plot 15 a viable explanation for why the flux is so low (Holzapfel-Pschorn 1986; Joabsson et al. 1999; Ström et al. 2005; Olefeldt et al. 2013; Schlesinger and Bernhardt 2013).

Another possible explanation as to why the fluxes are low in plot 15 could be that there might be a higher level of oxidation taking place in this plot. The oxidation of CH_4 usually occurs as the CH_4 passes the oxic zone or the rhizosphere (Lombardi et al. 1997; Frenzel and Karofeld 2000). Several studies show that one of the primary controls on CH_4 emissions may be the oxidation taking place in the rhizosphere and oxic zone (Armstrong and Armstrong 1988; Frenzel and Karofeld 2000; Ström et al. 2005).

The study conducted by Ström et al. (2005) also emphasizes the importance of substrate availability, such as acetate, in the production of CH_4. This is also highlighted in several other studies (Saarinen et al. 1992; Chanton et al. 1995; Bellisario et al. 1999; Joabsson

et al. 1999; Joabsson and Christensen 2001). The availability of substrates for CH_4-producing bacteria is in turn largely controlled by the species composition at the location, as well as the size of their root-system (Saarinen et al. 1992; Chanton et al. 1995; Joabsson et al. 1999; Joabsson and Christensen 2001; Ström et al. 2005). Therefore, it might be speculated that variation in substrate availability may be another factor explaining the variations in CH_4 emissions between the plots and sites.

A similar pattern can also be observed in Storflaket, where certain plots within a site have notably higher fluxes of CH_4 compared to the other plots (Figure 7). At this site plots 13-16 have substantially higher fluxes compared to the other plots at the same site. These plots have a typical wet minerotrophic species composition with a dominating vegetation consisting of sedges such as *C. canescens, C. flacca and E. angustifolium* (Appendix A, Table S3) (Svensson et al. 1999). Additionally, these plots also have an AL < 1 m, as well as a quite high WTD. Plots 15 and 16 have one of the highest WTD and both have an AL < 1 m. However, plot 16 has a higher CH_4 flux out of the two. This may be due to the fact that plot 16 only consists of *E. angustifolium*, whereas plot 15 also has *C. flacca* present (Appendix A, Table S3). As previously argued, *E. angustifolium* is quite large and may therefore have more aerenchymateous tissue for transporting CH_4 through the oxic zone and into the atmosphere (Joabsson and Christensen 2001; Falk et al. 2014). *E. angustifolium* may also have a larger root-system, thereby contributing to a higher substrate availability for CH_4 production (Bellisario et al. 1999; Ström et al. 2005).

The correlation matrices can be used to give an indication of what may be driving the CH_4 emissions at the study sites (Figure 8). Overall, across the sites, the strongest significant correlations for the CH_4 emission appears to be with WTD and AL depth, apart from in Katterjokk. The weak correlation between CH_4 emission and AL depth is simply because there is no permafrost present at this site, and therefore also no AL. The water table at this site, however, is the highest between all sites, but still has a weak correlation to CH_4 emission (r-value = 0.23, p-value = 0.133). This suggests that the water availability might not be a limiting factor at this site. Furthermore, studies have indicated that after the water table reaches a certain threshold it no longer influences the amount of CH_4 emission (Zona et al. 2009).

The strong influence of the WTD on CH_4 emissions is also quite evident when looking at the results of the wet and dry plots (Figure 9). The CH_4 fluxes seen in the wet plots are significantly higher than in the dry plots. This links well to the results between the sites and the individual plots within the three sites (Figure 5-7) since the plots with a higher water table often were accompanied by high CH_4 fluxes. The separation of all the plots into wet vs. dry made these differences become very clear, as the wet plots

had very high fluxes and the dry plots had fluxes around zero. As previously argued, a higher water table leads to more anoxic conditions (due to a larger anoxic zone) and subsequently more CH_4 production and emission (Ström and Christensen 2007). Additionally, wet sites also provide a more favorable environment for growth of aerenchymateous vegetation, which transport CH_4 into the atmosphere (Joabsson and Christensen 2001; Falk et al. 2014).

Moreover, all other correlations with CH_4 emission are quite weak, except for one intermediate correlation between NEE and CH_4 emission in Katterjokk (r-value = -0.58, p-value = 0.019). Several studies have suggested that there may be a linkage between amount of carbon uptake (NEE) and the emissions of CH_4 (Saarinen et al. 1992; Chanton et al. 1995; Joabsson et al. 1999; Joabsson and Christensen 2001; Lai et al. 2014). An increasing uptake of carbon i.e., photosynthesis would increase the amount of biomass of the vegetation. This may both increase the aerenchymateous tissue and subsequently increase the transport of CH_4 into the atmosphere. In addition, it may also increase the below-ground biomass (roots) and therefore contribute to more substrate availability which in turn increases the production and transport of CH_4 (Holzapfel-Pschorn 1986; Saarinen et al. 1992; Chanton et al. 1995; Joabsson et al. 1999; Joabsson and Christensen 2001).

Saarinen et al. (1992) conducted a study where the allocation of biomass of *C. rostrata* was estimated. The study showed that up to 90 % of the biomass was stored below ground. Katterjokk has *C. rostrata* growing in several of the plots (Appendix A, Table S1). This may partly explain the correlation (r-value = -0.58, p-value = 0.019) between NEE and CH_4 in Katterjokk, as a greater below-ground biomass means more roots and root exudates for CH_4 production (Holzapfel-Pschorn 1986; Saarinen et al. 1992; Chanton et al. 1995; Joabsson et al. 1999; Joabsson and Christensen 2001). This relationship was not found in Kursflaket and Storflaket. At these two sites both the NEE and CH_4 are very low, compared to Katterjokk, which may be why there were no correlation between the two variables (Figure 8). The low correlations between two variables also suggests that carbon most likely is not a limiting factor for CH_4 emissions (Zona et al. 2009). This result is also supported by the findings of Zona et al. (2009), as no relationship between the NEE and CH_4 was found in this study either. Additionally, the lack of correlation between the NEE and CH_4 suggests that there are other main drivers, such as perhaps differences in microbial communities.

Furthermore, the sites in this study are undergoing a change as the permafrost is disintegrating and altering the topography and species composition (Svensson et al. 1999; Christensen et al. 2004; Ström and Christensen 2007; Olefeldt et al. 2013). This is why the plots in this study consist of a vegetation composition that is mixed and

therefore not necessarily the typical composition that should be at sites with no, intermediate or relatively stable permafrost. The sites therefore consist of vegetation that both have and lack aerenchyma. This may also be a contributing factor to why the relationship between NEE and CH_4 is not present in Kursflaket and Storflaket and only intermediate in Katterjokk. Furthermore, this may be a hint of how these relationships might look on larger scales and in more natural ecosystems. These relationships may only exist when looking at individual plots where the dominating vegetation is aerenchymateous and might not be true when looking at the ecosystem as a whole.

5.2. CO_2 fluxes

The CO_2 uptake (NEE) was significantly higher at Katterjokk, compared to Kursflaket and Storflaket (Figure 4). This is also evident when examining the individual plots at the three sites (Figure 5-7). Katterjokk has a negative NEE throughout all plots, whereas in Kursflaket and Storflaket there is a larger variation where certain plots are taking up CO_2 while others are a source. As previously mentioned, Katterjokk is the only site out of the three that has a complete loss of permafrost and therefore also has the highest water table (Table 1). Wetter locations, as opposed to dryer conditions, may provide a more favorable environment for vegetation growth. More vegetation increases the productiveness and in turn the NEE (Ström and Christensen 2007). The high CO_2 uptake in Katterjokk indicates this site may have a higher amount of productive vegetation which is enabling more uptake (Ström and Christensen 2007).

When comparing the plots with the highest CO_2 uptake (NEE) (plot 3 and 7) with the ones that have the lowest CO_2 uptake (plot 1-2 and 4) in Katterjokk, there is no substantial difference in the vegetation composition that may give an indication as to why the fluxes vary (Figure 5) (Appendix A, Table S1). All plots consist of a mix of shrubs (*A. polifolia*), sedges (*C. rostrata*) and moss (*Sphagnum spp.*). There could however be a difference in amount of green biomass between the plots which may be causing this variation in fluxes. A large quantity of green biomass would mean more photosynthesizing plants i.e., a higher productivity and subsequently a higher uptake of CO_2. The weight of green biomass was not measured in this study, but it could be speculated that differences in biomass may be an influencing factor on the magnitude in fluxes, as this relationship has been seen in several previous studies (Grogan and Chapin 2000; Ström and Christensen 2007; Ström et al. 2012).

One interesting observation concerning the NEE is plot 1 in Storflaket which has a net release of CO_2 that is substantially higher than the other plots at the site. This plot has a vegetation consisting of only shrubs (*B. nana and E. nigrum*), which falls in line with

the environmental conditions at the plot (AL = 51 cm below surface and no measurable WTD) indicating more dry conditions (Appendix A, Table S3). A plausible explanation could be that the dryer conditions would cause a less favorable environment for vegetation growth, thereby decreasing the abundance of green biomass, compared to wetter locations. This would in turn decrease the photosynthesis (GPP) in relation to the plant respiration (R_a), leading to a positive NEE. Interestingly, plot 6 has the same WTD and AL depth as plot 1, as well as a similar vegetation composition (*E. nigrum*), but has a net uptake of CO_2. This indicates that there might be another variable driving the fluxes of CO_2 at these plots. Perhaps there could be variations in microbial communities causing differences in R_h driving the fluxes of CO_2.

The CO_2 release (R_{eco}) is significantly higher in Kursflaket, compared to Katterjokk and Storflaket (Figure 5). This is also reflected in the individual plots of the three sites, as Kursflaket has an overall higher R_{eco}, compared to Katterjokk and Storflaket which have a lower R_{eco} throughout the plots (Figure 5-7). This result is slightly contradictory as one would expect Katterjokk i.e., the site with the highest CO_2 uptake and, as previously argued, the highest abundance of green biomass to also have the highest respiration. It could be speculated that since Kursflaket is currently undergoing permafrost disintegration there could be a higher proportion of R_h from microbes that are disintegrating the previously frozen carbon, compared to Katterjokk. Katterjokk has already undergone a complete disintegration of the permafrost and therefore most previously frozen carbon may have already been disintegrated and respired, consequently causing this site to have a smaller proportion of R_h. However, since only the total respiration (R_{eco}) was measured in this study, it is not possible to find out the exact proportions of R_h vs. R_a.

A closer examination of the individual plots in Kursflaket for R_{eco} shows that plots 1-7 have notably lower fluxes compared to plots 8-16, especially when comparing maximum and minimum values (Figure 6). Moreover, plots 1-7 are all dry plots i.e., no detectible water table, whereas plots 8-16 all have a water table present (Appendix A, Table S2). Normally sites with a higher water content should not have a higher R_{eco} than a dry site, as the wetness of the soil would cause anoxic condition and thereby less respiration (Schelesinger and Bernhardt 2013). Why this is nonetheless occurring at the plots in Kursflaket may be an indication of methanotrophic respiration, as the methanotrophs are oxidizing the CH_4 (White et al., unpubl.). Another plausible explanation for the higher fluxes seen at plots 8-16 could be that these plots may have a larger quantity of green biomass, compared to plots 1-7, thereby causing a higher R_{eco} (Grogan and Chapin 2000; Ström and Christensen 2007).

The correlations for R_{eco} and NEE can be used in order to gain an understanding of what the drivers of the release and uptake of CO_2 are (Figure 8). Overall, there does not appear to be any strong correlations between R_{eco} and NEE with any of the environmental parameters. There is however a strong negative correlation between R_{eco}, GPP and NEE, both when looking at all sites together and individually. This correlation is expected, as these variables are connected. A higher GPP indicates a higher CO_2 uptake by plants and in turn more biomass storage (above and below ground). As biomass is stored, CO_2 is also released through R_a. A higher GPP also stimulates root exudation, which in turn is consumed by microbes that respire (R_h) (Holzapfel-Pschorn 1986; Schaefer et al. 2012; Schelesinger and Bernhardt 2013)

The lack of correlation between the uptake (NEE) and release of CO_2 (R_{eco}) with the environmental parameters are somewhat contradictory to previous studies (Chimner and Cooper 2003; Riutta et al. 2007; Ström and Christensen 2007; Ström et al. 2012). The uptake (NEE) and release of CO_2 (R_{eco}) have been shown to be driven by the type of vegetation cover and abundance of green biomass, as well as environmental factors such as depth of AL, WTD, T_{air}, T_{soil}, contrary to the results of this study (Grogan and Chapin 2000; Chimner and Cooper 2003; Riutta et al. 2007; Ström and Christensen 2007; Ström et al. 2012).

The correlations between NEE and R_{eco} against WTD and AL depth were overall quite low (Figure 8). However, when examining the results of the wet and dry plots, the GPP seen in the wet plots are significantly higher than in the dry plots (Figure 9). This may indicate that WTD could be a significant environmental driver for the CO_2 fluxes after all, as the GPP is derived from the NEE and R_{eco}. An increased WTD (until a certain point), may provide a more favorable environment for vegetation growth and thereby in turn increase the GPP. This idea could be confirmed by a comparison of biomass against CO_2 fluxes. However, as previously mentioned, comparisons between green biomass and CO_2 fluxes cannot be made, as the biomass was not measured. However, relationships between NEE and green biomass have been found in previous studies, therefore it is not unlikely that a similar relationship would have been found in this study as well (Grogan and Chapin 2000; Ström and Christensen 2007; Ström et al. 2012).

Why this study did not have any direct correlations between the CO_2 fluxes and the measured environmental parameters could be that none of the parameters are a limiting factor for the CO_2 fluxes at these specific sites, indicating that there are other limiting factors that were not measured in this study. The WTD, T_{air}, T_{soil} may be at an optimal level for the respective sites, thereby not limiting the CO_2 fluxes.

5.3. The results in a larger perspective

The three study sites had quite varying magnitudes of fluxes. Katterjokk, the site with a complete permafrost loss, had significantly higher CH_4 fluxes compared to the other two sites which had a moderate and stable permafrost, respectively. Furthermore, Katterjokk had the highest level of R_{eco} and the highest CO_2 uptake in the form of NEE. The main drivers of CH_4 fluxes throughout the sites were WTD and AL depth, whereas no specific environmental parameter could be identified as the driver of CO_2 fluxes. Furthermore, the fluxes at the individual plots, however, revealed a more complex reality, as within the sites there were in some cases substantial variations in magnitude in carbon fluxes. In most cases, the plots with higher fluxes also had a higher water table and deeper AL, as well as presence of aerenchymateous vegetation.

Overall, there were notable variations between and within the sites, demonstrating that even within the Abisko region, there are considerable variations in fluxes and drivers between individual sites, as well as within. While there are numerous studies of the permafrost disintegration in certain well researched areas, such as Stordalen in Abisko, fewer studies have been done in areas outside of Stordalen (Svensson et al. 1999; Christensen et al. 2004; Ström and Christensen 2007; Jackowicz-Korczyński et al. 2010; Olefeldt and Roulet 2012). Furthermore, the results of the research conducted in Stordalen is in some cases also extrapolated for larger areas (Metcalf et al. 2018). This means that there is a generalization that areas outside of Stordalen behave in a similar manner. The results of this study have shown that the variations between sites and plots in the Abisko region can be significant.

5.4. Limitations

During the measurement period there was a few instances where the instrument used to measure the gas concentrations malfunctioned. The measurements taken at these particular times were unusable, and thereby excluded from this study. This may have influenced the calculation of the fluxes. This influence, however, is most likely quite small and non-significant for the overall results of the study.

Due to time limitations, calculations of RMSE, to conclude whether or not low fluxes accompanied by a low r^2 were usable, were only conducted on a small subset of the data. It was then assumed, based on the RMSE of the subset, that all low fluxes with low r^2-value were usable. However, if time allowed calculations of RMSE would have been performed on all low fluxes with a low r^2-value and not only a subset, in order to get a comprehensive idea of the uncertainty in the measurements. Another option to

deal with the measurement uncertainty would have been to determine a threshold r^2-value such as in the study conducted by Lai et al. (2014). In this study a threshold of the r^2-value was set and values below this threshold were deemed as being low quality fluxes and thereby discarded from the study.

Measurements of biomass, such as dry weight of green biomass, would have contributed to this study, as it would have helped strengthen the arguments made on whether or not there was a relationship between biomass and the carbon fluxes. Furthermore, in order to support the theories made about the presence or lack of substrates as a driver of carbon fluxes, measurements of concentration of compounds would have contributed to the results of this study.

Finally, in order to get a more robust data set and account for the large variability between the plots, a higher amount of replicate measurements could have been taken. This would have been especially beneficial at the wet sites and plots, as these tend to have a larger variability compared to dry sites and plots, as seen in figure 5-7.

6. Conclusion

The aim of this study was to investigate the influence of the stage of permafrost degradation and landscape variability on the magnitude of carbon fluxes (CO_2/CH_4) by relating the fluxes to presence of aerenchymateous vegetation, AL depth and WTD. This study showed that there were significant variations in CH_4 and CO_2 fluxes between the sites. However, it was clear that Katterjokk, with a complete permafrost loss, had substantially higher CH_4 emissions as well as a higher CO_2 uptake compared to the other two sites. This difference in magnitude of CH_4 flux was shown to be mainly driven by the WTD and AL depth, as well as the abundance of aerenchymateous vegetation, as hypothesized. This was evident when examining the individual plots of the sites as well as the wet and dry plots. The drivers of the CO_2 fluxes were not as straightforward as for the CH_4 fluxes. There was a lack of significant correlations between the CO_2 fluxes and environmental drivers throughout the sites, however the wet and dry plots indicated that there may be a connection between WTD and CO_2, although not as clearly as for the CH_4 fluxes.

The Abisko region is undergoing major changes as the permafrost is disintegrating and thereby causing substantial spatial variation across the area. As a result of the spatial variability of site-specific conditions, there are considerable variations in carbon fluxes between and within the three study sites, as demonstrated by the results of this study. The differences in carbon fluxes and the site-specific conditions are important to take

into consideration when extrapolating and generalising for larger areas. Furthermore, a continued disintegration of permafrost and deepening of the AL, as projected by the IPCC (2019), may further alter the sub arctic ecosystem of Abisko and thereby enhance the spatial variability, as environmental conditions continue to change. In addition, further permafrost disintegration will lead to even more emissions of CH_4 and CO_2, amplifying the initial warming (Johansson et al. 2006; Dean et al. 2018; IPCC 2019).

References

Aphalo, J.P. 2021. ggpmisc: Miscellaneous Extensions to 'ggplot2'. R package version 0.3.8-1.

Armstrong, J., and W. Armstrong. 1988. Phragmites australis–A preliminary study of soil-oxidizing sites and internal gas transport pathways. *New phytologist,* 108**:** 373-382.

Bellisario, L., J. Bubier, T. Moore, and J. Chanton. 1999. Controls on CH4 emissions from a northern peatland. *Global Biogeochemical Cycles,* 13**:** 81-91.

Biskaborn, B. K., S. L. Smith, J. Noetzli, H. Matthes, G. Vieira, D. A. Streletskiy, P. Schoeneich, V. E. Romanovsky, et al. 2019. Permafrost is warming at a global scale. *Nature communications,* 10**:** 1-11.

Callaghan, T. V., C. Jonasson, T. Thierfelder, Z. Yang, H. Hedenås, M. Johansson, U. Molau, R. Van Bogaert, et al. 2013. Ecosystem change and stability over multiple decades in the Swedish subarctic: complex processes and multiple drivers. *Philosophical Transactions of the Royal Society B: Biological Sciences,* 368**:** 20120488.

Chanton, J. P., J. E. Bauer, P. A. Glaser, D. I. Siegel, C. A. Kelley, S. C. Tyler, E. H. Romanowicz, and A. Lazrus. 1995. Radiocarbon evidence for the substrates supporting methane formation within northern Minnesota peatlands. *Geochimica et Cosmochimica Acta,* 59**:** 3663-3668.

Chimner, R. A., and D. J. Cooper. 2003. Influence of water table levels on CO2 emissions in a Colorado subalpine fen: an in situ microcosm study. *Soil Biology and Biochemistry,* 35**:** 345-351.

Christensen, T. R., T. Johansson, H. J. Åkerman, M. Mastepanov, N. Malmer, T. Friborg, P. Crill, and B. H. Svensson. 2004. Thawing sub-arctic permafrost: Effects on vegetation and methane emissions. *Geophysical research letters,* 31.

Dean, J. F., J. J. Middelburg, T. Röckmann, R. Aerts, L. G. Blauw, M. Egger, M. S. Jetten, A. E. de Jong, et al. 2018. Methane feedbacks to the global climate system in a warmer world. *Reviews of Geophysics,* 56**:** 207-250.

de Mendiburu, F. 2020. agricolae: Statistical Procedures for Agricultural Research. R package version 1.3-3.

Dobinski, W. 2011. Permafrost. *Earth-Science Reviews,* 108**:** 158-169.

Falk, J. M., N. M. Schmidt, T. R. Christensen, and L. Ström. 2015. Large herbivore grazing affects the vegetation structure and greenhouse gas balance in a high arctic mire. *Environmental Research Letters,* 10**:** 045001.

Falk, J. M., N. M. Schmidt, and L. Ström. 2014. Effects of simulated increased grazing on carbon allocation patterns in a high arctic mire. *Biogeochemistry,* 119**:** 229-244.

Fischer, H., A. Meyer, K. Fischer, and Y. Kuzyakov. 2007. Carbohydrate and amino acid composition of dissolved organic matter leached from soil. *Soil Biology and Biochemistry,* 39**:** 2926-2935.

Frenzel, P., and E. Karofeld. 2000. CH4 emission from a hollow-ridge complex in a raised bog: The role of CH4 production and oxidation. *Biogeochemistry,* 51**:** 91-112.

Fyfe, J. C., K. Von Salzen, N. P. Gillett, V. K. Arora, G. M. Flato, and J. R. McConnell. 2013. One hundred years of Arctic surface temperature variation due to anthropogenic influence. *Scientific Reports,* 3**:** 1-7.

Gisnås, K., B. Etzelmüller, C. Lussana, J. Hjort, A. B. K. Sannel, K. Isaksen, S. Westermann, P. Kuhry, et al. 2017. Permafrost map for Norway, Sweden and Finland. *Permafrost and periglacial processes,* 28**:** 359-378.

Grogan, P., and F. Chapin Iii. 2000. Initial effects of experimental warming on above- and belowground components of net ecosystem CO 2 exchange in arctic tundra. *Oecologia,* 125**:** 512-520.

Gruber, S. 2012. Derivation and analysis of a high-resolution estimate of global permafrost zonation. *The Cryosphere,* 6**:** 221-233.

Hall, A. 2004. The role of surface albedo feedback in climate. *Journal of Climate,* 17**:** 1550-1568.

Hamner, B., and M. Frasco. 2018. Metrics: Evaluation Metrics for Machine Learning. R package version 0.1.4.

Harrell Jr, F. E. 2021. Hmisc: Harrell Miscellaneous. R package version 4.5-0.

Hawkins, E., and R. Sutton. 2012. Time of emergence of climate signals. *Geophysical Research Letters,* 39.

Holzapfel-Pschorn, A., R. Conrad, and W. Seiler. 1986. Effects of vegetation on the emission of methane from submerged paddy soil. *Plant and soil,* 92**:** 223-233.

IPCC Meredith, M., M. Sommerkorn, S. Cassotta, C. Derksen, A. Ekaykin, A. Hollowed, G. Kofinas, A. Mackintosh, et al. 2019. Polar Regions. Chapter 3, IPCC Special Report on the Ocean and Cryosphere in a Changing Climate.

Jackowicz-Korczyński, M., T. R. Christensen, K. Bäckstrand, P. Crill, T. Friborg, M. Mastepanov, and L. Ström. 2010. Annual cycle of methane emission from a subarctic peatland. *Journal of Geophysical Research: Biogeosciences,* 115.

Joabsson, A., and T. R. Christensen. 2001. Methane emissions from wetlands and their relationship with vascular plants: an Arctic example. *Global Change Biology,* 7**:** 919-932.

Joabsson, A., T. R. Christensen, and B. Wallén. 1999. Vascular plant controls on methane emissions from northern peatforming wetlands. *Trends in Ecology & Evolution,* 14**:** 385-388.

Johansson, M., T. R. Christensen, H. J. Akerman, and T. V. Callaghan. 2006. What determines the current presence or absence of permafrost in the Torneträsk region, a sub-arctic landscape in northern Sweden? *AMBIO: A Journal of the Human Environment,* 35**:** 190-197.

Johansson, M., J. Åkerman, F. Keuper, T. R. Christensen, H. Lantuit, and T. V. Callaghan. 2011. Past and present permafrost temperatures in the Abisko area: Redrilling of boreholes. *Ambio,* 40**:** 558-565.

Kassambara, A. 2020. ggpubr: 'ggplot2' Based Publication Ready Plots. R package version 0.4.0.

Kotsyurbenko, O. R., K. J. Chin, M. V. Glagolev, S. Stubner, M. V. Simankova, A. N. Nozhevnikova, and R. Conrad. 2004. Acetoclastic and hydrogenotrophic methane production and methanogenic populations in an acidic West-Siberian peat bog. *Environmental microbiology,* 6**:** 1159-1173.

Kujala, K., M. Seppälä, and T. Holappa. 2008. Physical properties of peat and palsa formation. *Cold Regions Science and Technology,* 52**:** 408-414.

Lai, D. Y., N. T. Roulet, and T. R. Moore. 2014. The spatial and temporal relationships between CO2 and CH4 exchange in a temperate ombrotrophic bog. *Atmospheric Environment,* 89**:** 249-259.

Lindgren, A., G. Hugelius, and P. Kuhry. 2018. Extensive loss of past permafrost carbon but a net accumulation into present-day soils. *Nature,* 560**:** 219-222.

Loisel, J., Z. Yu, D. W. Beilman, P. Camill, J. Alm, M. J. Amesbury, D. Anderson, S. Andersson, et al. 2014. A database and synthesis of northern peatland soil properties and Holocene carbon and nitrogen accumulation. *the Holocene,* 24**:** 1028-1042.

Lombardi, J. E., M. A. Epp, and J. P. Chanton. 1997. Investigation of the methyl fluoride technique for determining rhizospheric methane oxidation. *Biogeochemistry,* 36**:** 153-172.

MacDonald, G. M., D. W. Beilman, K. V. Kremenetski, Y. Sheng, L. C. Smith, and A. A. Velichko. 2006. Rapid early development of circumarctic peatlands and atmospheric CH4 and CO2 variations. *science,* 314**:** 285-288.

Malmer, N., T. Johansson, M. Olsrud, and T. R. Christensen. 2005. Vegetation, climatic changes and net carbon sequestration in a North-Scandinavian subarctic mire over 30 years. *Global Change Biology,* 11**:** 1895-1909.

Matson, P. A., and R. C. Harriss. 2009. *Biogenic trace gases: measuring emissions from soil and water*. John Wiley & Sons.

McCalley, C. K., B. J. Woodcroft, S. B. Hodgkins, R. A. Wehr, E.-H. Kim, R. Mondav, P. M. Crill, J. P. Chanton, et al. 2014. Methane dynamics regulated by microbial community response to permafrost thaw. *Nature,* 514**:** 478-481.

Metcalfe, D. B., T. D. Hermans, J. Ahlstrand, M. Becker, M. Berggren, R. G. Björk, M. P. Björkman, D. Blok, et al. 2018. Patchy field sampling biases understanding of climate change impacts across the Arctic. *Nature ecology & evolution,* 2**:** 1443-1448.

Natali, S. M., E. A. Schuur, M. Mauritz, J. D. Schade, G. Celis, K. G. Crummer, C. Johnston, J. Krapek, et al. 2015. Permafrost thaw and soil moisture driving CO2 and CH4 release from upland tundra. *Journal of Geophysical Research: Biogeosciences,* 120**:** 525-537.

Nisbet, E. G., E. J. Dlugokencky, and P. Bousquet. 2014. Methane on the rise—again. *Science,* 343**:** 493-495.

Olefeldt, D., and N. T. Roulet. 2012. Effects of permafrost and hydrology on the composition and transport of dissolved organic carbon in a subarctic peatland complex. *Journal of Geophysical Research: Biogeosciences,* 117.

Olefeldt, D., M. R. Turetsky, P. M. Crill, and A. D. McGuire. 2013. Environmental and physical controls on northern terrestrial methane emissions across permafrost zones. *Global Change Biology,* 19**:** 589-603.

Ovenden, L. 1990. Peat accumulation in northern wetlands. *Quaternary research,* 33**:** 377-386.

Riutta, T., J. Laine, and E.-S. Tuittila. 2007. Sensitivity of CO 2 exchange of fen ecosystem components to water level variation. *Ecosystems,* 10**:** 718-733.

Romanovsky, V., K. Isaksen, D. Drozdov, O. Anisimov, A. Instanes, M. Leibman, A. McGuire, N. Shiklomanov, et al. 2017. Changing permafrost and its impacts. *Snow, Water, Ice and Permafrost in the Arctic (SWIPA),* 2017**:** 65-102.

Rydin, H., P. Snoeijs, and M. Diekmann. 1999. *Swedish plant geography: dedicated to Eddy van der Maarel on his 65th birthday*. Svenska växtgeografiska sällsk.

Saarinen, T., K. Tolonen, and H. Vasander. 1992. Use of 14C labelling to measure below-ground biomass of mire plants. *Suo,* 43**:** 245-247.

Sælthun, N. R., and L. Barkved. 2003. Climate change scenarios for the SCANNET region.

Saunois, M., A. R. Stavert, B. Poulter, P. Bousquet, J. G. Canadell, R. B. Jackson, P. A. Raymond, E. J. Dlugokencky, et al. 2020. The global methane budget 2000–2017. *Earth System Science Data,* 12**:** 1561-1623.

Schaefer, H., S. E. M. Fletcher, C. Veidt, K. R. Lassey, G. W. Brailsford, T. M. Bromley, E. J. Dlugokencky, S. E. Michel, et al. 2016. A 21st-century shift from fossil-fuel to biogenic methane emissions indicated by 13CH4. *Science,* 352**:** 80-84.

Schaefer, K., C. R. Schwalm, C. Williams, M. A. Arain, A. Barr, J. M. Chen, K. J. Davis, D. Dimitrov, et al. 2012. A model-data comparison of gross primary productivity: Results from the North American Carbon Program site synthesis. *Journal of Geophysical Research: Biogeosciences,* 117.

Schlesinger, W., and E. Bernhardt. 2013. Wetland ecosystems. *Biogeochemistry, Academic Press, Oxford, UK***:** 233-274.

Schutz, H. 1991. Role of plants in regulating the methane flux to the atmosphere. *Trace Gas Emission by Plants***:** 29-63.

Schuur, E. A., B. Abbott, W. Bowden, V. Brovkin, P. Camill, J. Canadell, J. Chanton, F. Chapin, et al. 2013. Expert assessment of vulnerability of permafrost carbon to climate change. *Climatic Change,* 119**:** 359-374.

Schuur, T., A. D. McGuire, V. E. Romanovsky, C. Schadel, and M. Mack. 2018. Arctic and boreal carbon.

Seppälä, M. 1982. An experimental study of the formation of palsas. In *Proceedings Fourth Canadian Permafrost Conference, Calgary. National Research Council of Canada, Ottawa,* 36-42.

Seppälä, M. 2006. Palsa mires in Finland. *The finnish environment,* 23**:** 155-162.

Serreze, M. C., and J. A. Francis. 2006. The Arctic amplification debate. *Climatic change,* 76**:** 241-264.

Ström, L., and T. R. Christensen. 2007. Below ground carbon turnover and greenhouse gas exchanges in a sub-arctic wetland. *Soil Biology and Biochemistry,* 39**:** 1689-1698.

Ström, L., M. Mastepanov, and T. R. Christensen. 2005. Species-specific effects of vascular plants on carbon turnover and methane emissions from wetlands. *Biogeochemistry,* 75**:** 65-82.

Ström, L., T. Tagesson, M. Mastepanov, and T. R. Christensen. 2012. Presence of Eriophorum scheuchzeri enhances substrate availability and methane emission in an Arctic wetland. *Soil Biology and Biochemistry,* 45**:** 61-70.

Svensson, B., T. Christensen, E. Johansson, and M. Öquist. 1999. Interdecadal changes in CO 2 and CH 4 fluxes of a subarctic mire: Stordalen revisited after 20 years. *Oikos***:** 22-30.

Tarnocai, C., J. Canadell, E. A. Schuur, P. Kuhry, G. Mazhitova, and S. Zimov. 2009. Soil organic carbon pools in the northern circumpolar permafrost region. *Global biogeochemical cycles,* 23.

Torn, M. S., and F. S. Chapin III. 1993. Environmental and biotic controls over methane flux from arctic tundra. *Chemosphere,* 26**:** 357-368.

Walvoord, M. A., and B. L. Kurylyk. 2016. Hydrologic impacts of thawing permafrost—A review. *Vadose Zone Journal,* 15.

Wang, Z., D. Zeng, and W. H. Patrick. 1996. Methane emissions from natural wetlands. *Environmental Monitoring and Assessment,* 42**:** 143-161.

Wei, T., and V. Simko. 2017. Corrplot: Visualization of a Correlation Matrix. R package version version 0.84.

Wickham, H. ggplot2: Elegant Graphics for Data Analysis. Springer-Verlag New York. 2016.

Wickham, H., R. François, L. Henry and K. Müller. 2021. dplyr: A Grammar of Data Manipulation. R package version 1.0.4.

Zona, D., W. Oechel, J. Kochendorfer, K. Paw U, A. Salyuk, P. Olivas, S. Oberbauer, and D. Lipson. 2009. Methane fluxes during the initiation of a large-scale water table manipulation experiment in the Alaskan Arctic tundra. *Global Biogeochemical Cycles,* 23.

Åkerman, H. J., and M. Johansson. 2008. Thawing permafrost and thicker active layers in sub-arctic Sweden. *Permafrost and periglacial processes,* 19**:** 279-292.

Appendix A

Table S1. Table showing the vegetation composition, AL depth (cm below surface) and WTD (cm below surface) for each plot in Katterjokk. AL depth and WTD are mean values of the five replicate measurements taken at each plot.

	Katterjokk		
	Vegetation	**AL**	**WTD**
Plot 1	*Andromeda polifolia, Carex rostrata, Eleocharis quinqueflora, Sphagnum spp.*	>100	-1.6
Plot 2	*Andromeda polifolia, Carex rostrata, Eleocharis quinqueflora (few), Sphagnum spp.*	>100	-9.02
Plot 3	*Andromeda polifolia, Carex rostrata, Eleocharis quinqueflora, Sphagnum spp., Vaccinium oxycoccos*	>100	-9.2
Plot 4	*Andromeda polifolia, Carex lasiocarpa, Carex rostrata, Salix, Sphagnum spp., Vaccinium oxycoccos*	>100	-8.44
Plot 5	*Andromeda polifolia, Carex rostrata (dominating), Sphagnum spp.*	>100	-8.86
Plot 6	*Andromeda polifolia, Carex rostrata, Carex rariflora, Eleocharis quinqueflora, Sphagnum spp.*	>100	-11.06
Plot 7	*Andromeda polifolia, Carex rostrata, Eleocharis quinqueflora, Sphagnum spp.*	>100	-9.26
Plot 8	*Carex rostrata (few), Eleocharis quinqueflora, Sphagnum spp.*	>100	-8.3

Table S2. Table showing the vegetation composition, AL depth (cm below surface) and WTD (cm below surface) for each plot in Kursflaket. AL depth and WTD are mean values of the five replicate measurements taken at each plot. NA-values for the WTD indicates a dry plot and therefore no WTD could be measured.

	Kursflaket		
	Vegetation	**AL**	**WTD**
Plot 1	*Andromeda polifolia, Betula nana, Empetrum nigrum*	46.4	NA
Plot 2	*Betula nana, Empetrum nigrum, Eriophorum vaginatum*	47	NA
Plot 3	*Andromeda polifolia, Empetrum nigrum, Rubus chamaemorus*	47.6	NA
Plot 4	*Empetrum nigrum, Eriophorum vaginatum, Rubus chamaemorus, Vaccinium uliginosum*	47	NA
Plot 5	*Empetrum nigrum, Eriophorum vaginatum, Vaccinium uliginosum*	47	NA
Plot 6	*Betula nana, Empetrum nigrum*	47.4	NA
Plot 7	*Betula nana, Carex spp., Cladina, Sphagnum spp.*	61	-31.4
Plot 8	*Andromeda polifolia, Sphagnum spp.*	55	-38.8
Plot 9	*Empetrum nigrum, Sphagnum spp.*	55	-27
Plot 10	*Carex chordorrhiza, Empetrum nigrum, Rubus chamaemorus*	87.8	-22.2
Plot 11	*Andromeda polifolia, Betula nana, Carex chordorrhiza*	65	-23
Plot 12	*Andromeda polifolia, Carex chordorrhiza, Salix*	78	-23.3
Plot 13	*Andromeda polifolia, Carex bigelowii, Eriophorum angustifolium*	>100	-9.16
Plot 14	*Andromeda polifolia, Carex bigelowii, Eriophorum angustifolium*	>100	-9.4
Plot 15	*Andromeda polifolia, Carex bigelowii, Carex chordorrhiza*	>100	-11.6
Plot 16	*Andromeda polifolia, Carex bigelowii, Empetrum nigrum*	58.6	-27.8

Table S3. Table showing the vegetation composition, AL depth (cm below surface) and WTD (cm below surface) for each plot in Storflaket. AL depth and WTD are mean values of the five replicate measurements taken at each plot. NA-values for the WTD indicates a dry plot and therefore no WTD could be measured.

	Storflaket		
	Vegetation	**AL**	**WTD**
Plot 1	*Betula nana, Empetrum nigrum*	51	NA
Plot 2	*Empetrum nigrum, Eriophorum vaginatum*	52.4	NA
Plot 3	*Empetrum nigrum, Eriophorum vaginatum*	55.8	NA
Plot 4	*Empetrum nigrum, Eriophorum vaginatum*	50	NA
Plot 5	*Betula nana, Empetrum nigrum*	46	NA
Plot 6	*Empetrum nigrum*	50	NA
Plot 7	*Empetrum nigrum, Rubus chamaemorus*	80.2	NA
Plot 8	*Betula nana, Carex spp., Rubus chamaemorus*	>100	NA
Plot 9	*Eriophorum angustifolium (small), Sphagnum spp.*	96.4	-32.34
Plot 10	*Andromeda polifolia, Eriophorum vaginatum, Rubus chamaemorus, Sphagnum spp.*	79.4	NA
Plot 11	*Empetrum nigrum, Eriophorum vaginatum*	65.6	NA
Plot 12	*Andromeda polifolia, Betula nana, Sphagnum spp.*	79.8	NA
Plot 13	*Carex canescens*	>100	-11.88
Plot 14	*Carex flacca, Eriophorum angustifolium*	>100	-6
Plot 15	*Carex flacca, Eriophorum angustifolium*	>100	-3.66
Plot 16	*Eriophorum angustifolium*	>100	-3.96